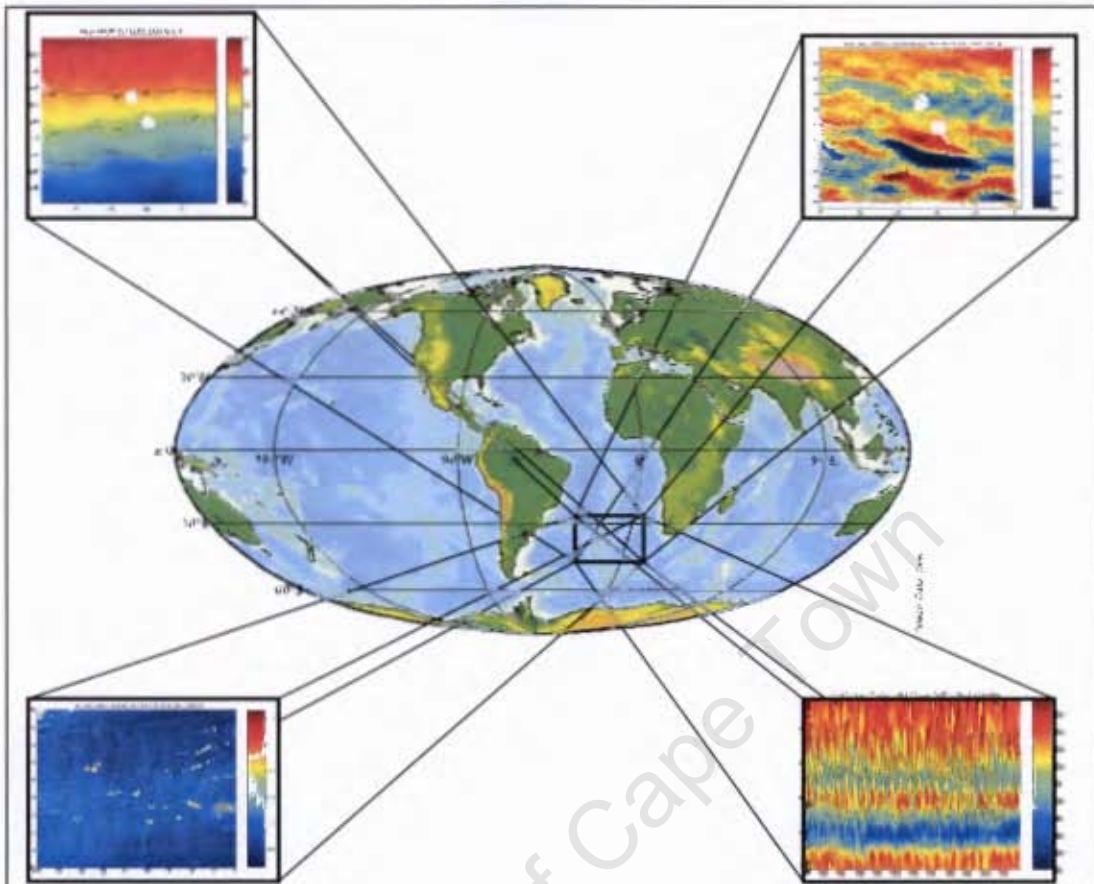


The copyright of this thesis vests in the author. No quotation from it or information derived from it is to be published without full acknowledgement of the source. The thesis is to be used for private study or non-commercial research purposes only.

Published by the University of Cape Town (UCT) in terms of the non-exclusive license granted to UCT by the author.



## On the Subtropical Front in the South Atlantic Ocean

Michael Funke  
FNKMIC001



A Dissertation Submitted In Fulfillment Of The Requirements For The Degree of Master In Science

In The Division of Physical Oceanography, Department of Oceanography,

Science Faculty, University Of Cape Town.

Cape Town, October 2009

## CONTENTS

---

Abstract	i
Acknowledgements	ii
List of Abbreviations	iii
List of Tables	iv
List of Figures	iv
<b>CHAPTER 1: INTRODUCTION</b>	<b>1</b>
1.1. Introduction	1
1.2. Subtropical Convergence/Front/Frontal Zone	2
1.2.1. Discrepancy about use of term	2
1.2.2. Criteria for surface STF identification	3
1.3. General circulation of the South Atlantic	4
1.3.1. STF in the South Atlantic	4
1.3.2. The South Atlantic Current	8
1.4. Previous studies in the Central South Atlantic Region	9
1.4.1. Physical oceanographic studies	9
1.4.2. Geological and Biological oceanographic studies	12
1.4.3. Satellite derived oceanographic studies	15
1.5. Study Aims	18
<b>CHAPTER 2: DATA and METHODS</b>	<b>19</b>
2.1. Data sources and characteristics	21
2.1.1. Gough Island in-situ SST data	21
2.1.2. NOAA OISST v.2 data	21
2.1.3. AMSR-E SST data	22
2.1.4. AVISO geostrophic current data	24
2.1.5. SODA model data	25
2.1.6. Etopo2 bathymetry data	26
2.1.7. Live Access Server (LAS) Websites	26
2.2. Methods	27
2.2.1. Calculations of associated means, anomalies	27
2.2.1.1. Monthly, yearly and overall means	27
2.2.1.2. Anomaly and normalised anomaly calculations	28
2.2.1.3. Latitudinal temperature gradients in °C/km	28
<b>CHAPTER 3: RESULTS</b>	<b>29</b>
3.1. Introduction to Region of Interest	29
3.1.1. Mean SST	29
3.1.2. Mean sub-surface temperature, salinity and U-current component	32
3.1.3. Mean circulations	37
3.2. Can we ascertain the seasonality of the STF from OISST and AMSR data?	39
3.3. How well do SODA model currents compare to AVISO geostrophic currents in the central South Atlantic?	44
3.4. What caused the cold event of 1992?	50
<b>CHAPTER 4: DISCUSSION and CONCLUSION</b>	<b>56</b>
4.1.1. Can we ascertain the seasonality of the STF from OISST and AMSR data?	56
4.1.2. How well do SODA model currents compare to AVISO geostrophic currents in the central South Atlantic?	58
4.1.3. What caused the cold event of 1992?	60
4.2. Conclusions	61
<b>REFERENCES</b>	<b>64</b>
<b>APPENDIX</b>	<b>74</b>

**In Memory of**

**Wolfgang Funke**

\*04/12/1919

† 21/02/2006

**and**

**Hannelore Funke**

\*10/10/1921

† 25/06/2008

*My Legendary Grandparents*

University of Cape Town

## Abstract

The region surrounding the Tristan da Cunha Archipelago has received little attention to date due to its remote location. An extensive revision of previous literature covers the majority of oceanographic research undertaken in the region of interest. New satellite derived oceanographic data sets and the SODA Reanalysed model are used to overcome the sparse extent of in-situ data in this region. Using latitudinal temperature gradients to track the surface expression of the Subtropical Front from AMSR and OISST satellite derived sea surface temperature data reveals consistencies with previous literature. A latitudinal rate of change of  $0.012^{\circ}\text{C}/\text{km}$  is found to best represent the surface expression of the STF. Comparing AVISO derived geostrophic currents with SODA Reanalysed model simulated currents over a 13 year period is performed. Investigation of a cold event at the Tristan da Cunha Archipelago reveals a possible link to El Niño dependent wind anomalies. There is no evidence of the STF moving north to create such a cold event. The emerging potential of satellite derived data and model simulations will greatly increase the understanding of remote places, but models will first need to improve in the Mid-South Atlantic sector.

## **Acknowledgements**

I would firstly like to thank Dr Mathieu Rouault for his guidance through the last 3 years, and great help with all the data sets. Thank you to Dr Isabelle Ansorge whose door was always open. Thank you also to NRF for the financial support.

A further thank you to my office partners Björn Backeberg and Neil Swart who always willing to answer questions and helped with the wonders of MatLab. Thank you for tolerating me. Further away, outside the Oceanography Department, I would like to thank my parents for their unwavering support. Finally, a massive thanks goes out to all the people who supported me during the final few tough months, your distractions helped immensely to keep me on track. A special mention to Neil, Björn, Toby, Seb, Donovan and Patrick.

University of Cape Town

## List of Abbreviations

AABW	Antarctic Bottom Water
AAIW	Antarctic Intermediate water
ACC	Antarctic Circumpolar Current
ADCP	Acoustic Doppler Current Profiler
AMSR	Advanced Microwave Scanning Radiometer
AMO	Atlantic Multidecadal Oscillation
AVISO data	Archiving Validation and Interpretation of Satellite Oceanographic data
BMC	Brazil/Malvinas Confluence
CTDO	Conductivity Temperature Depth Oxygen
ENSO	El Niño Southern Oscillation
JFM	January February March
JAS	July August September
MSLP	Mean Sea Level Pressure
NADW	North Atlantic Deep Water
NCAR	National Centre for Atmospheric Research
NCEP	National Centres for Environmental Prediction
NNR	NCEP-NCAR Reanalysis
NOAA	National Ocean and Atmosphere Administration
NSTF	Northern Subtropical Front
OISST	Optimally Interpolated Sea Surface Temperature
ONI	Oceanic Niño Index
REMSS	Remote Sensing Systems
SAC	South Atlantic Current
SACW	South Atlantic Central Water
SACZ	South Atlantic Convergence Zone
SAF	Sub Antarctic Front
SAM	Southern Annular Mode
SAO	Semi-Annual Oscillation
SASW	Sub Antarctic Surface Water
SAWB	South African Weather Bureau
SLH	Sea Level Height
SLP	Sea Level Pressure
SODA	Simple Ocean Data Assimilation
SSH	Sea Surface Height
SST	Sea Surface Temperature
SSTF	Southern Subtropical Front
STC	Subtropical Convergence
STF	Subtropical Front
STFZ	Subtropical Frontal Zone
TRMM	Tropical Rainfall Measuring Mission
WOCE	World Ocean Circulation Experiment
XBT	Expendable Bathythermograph

## List of Tables

<u>Table 1</u> Criteria for STF identification (adapted from Belkin and Gordon, 1996)	3
<u>Table 2</u> Details for WOCE lines within the enclosed area in Figure 3 above	20
<u>Table 3</u> Anomalous SST events at the Tristan da Cunha Archipelago	51

## List of Figures

<u>Figure 1</u> The position of the fronts and large-scale circulation in the South Atlantic Ocean (Smythe-Wright <i>et al.</i> , 1998), with the Tristan Archipelago and the Brazil/Malvinas Confluence (BMC) identified.	6
<u>Figure 2</u> The Region of Interest centred on the Tristan da Cunha Archipelago, hereafter depicted as white triangles, showing their location to the east of the prominent Mid-Atlantic Ridge.	8
<u>Figure 3</u> Temperature-Salinity diagram for the waters present in the South Atlantic Ocean. The shaded region depicts the possible location of the STF (From Sverdrup <i>et al.</i> , 1942)	13
<u>Figure 4</u> Compilation of World Ocean Circulation Experiment (WOCE, blue) lines and South Atlantic Ventilation Experiment (SAVE, yellow) lines in the South Atlantic available in the WOCE and SAVE database at the end of the 20 <sup>th</sup> century highlighting the sparseness of data in the Region of Interest (represented by the enclosed area). Tristan da Cunha (north) and Gough Island (south) are shown by white triangles.	20
<u>Figure 5</u> Mean SST in °C for OISST data (a) and AMSR data (b) for January 2004 in a region downstream of Tristan da Cunha, highlighting the higher spatial resolution of the AMSR data over the OISST data, which has the higher temporal resolution.	23
<u>Figure 6</u> Mean SST in °C for January, February and March (a) and July, August and September (b) from AMSR SST data for the period 2002-2006. The data is described in Chapter 2. The white areas are Tristan da Cunha (north) and Gough Island (south).	30
<u>Figure 7</u> Mean monthly SST in °C for Tristan da Cunha (blue) and Gough Island (black) from 24 years of OISST data with bars depicting standard deviations.	31
<u>Figure 8</u> Mean sub-surface SODA temperature data in °C at 15°W for a) total water column, b) top 1000m and c) top 200m	33
<u>Figure 9</u> Mean sub-surface SODA salinity data in psu at 15°W a) total water column, b) top 1000m and c) top 200m	35
<u>Figure 10</u> Mean sub-surface SODA U-current component data in m/s at 15°W for a) total water column, b) top 1000m and c) top 200m	36



<u>Figure 11</u> Mean AVISO absolute geostrophic current in cm/s for January, February and March (a) and July, August and September (b), highlighting the broad zone difference of current strength in the region. Tristan da Cunha (north) and Gough Island (south) are shown by white triangles.	38
<u>Figure 12</u> Mean AVISO absolute geostrophic current in cm/s for points situated at Tristan da Cunha (top) and Gough Island (bottom)	39
<u>Figure 13</u> OISST comparison with in-situ Gough Island SST for 1982-2005 (a) and seasonal mean (b)	40
<u>Figure 14</u> Hovmöller plot of OISST latitudinal temperature gradient for 1982 to 2005 overlaid with isotherms assigned to STF temperature ranges, highlighting the stable seasonal signal	41
<u>Figure 15</u> Hovmöller plot of AMSR latitudinal temperature gradient for 2003 to 2006 overlaid with isotherms assigned to STF temperature ranges	42
<u>Figure 16</u> Mean latitudinal AMSR SST gradient overlaid with AVISO derived current data. The white areas are Tristan da Cunha (north) and Gough Island (south).	43
<u>Figure 17</u> 1 month (top); 3 month (middle); and 12month (bottom) mean AVISO derived geostrophic currents in cm/s for 1993	44
<u>Figure 18</u> Mean AVISO derived geostrophic current for period 1993-2005 at the Tristan da Cunha Archipelago with Etopo2 bathymetry as background. The light green area on the left side in the Figure represents the Mid-Atlantic Ridge, while the white triangle in the centre incorporates Tristan da Cunha, Nightingale and Inaccessible Islands. The dark orange regions on the right are shallow seamounts. On average, the depth in the region of interest is in excess of 3000m, depicted as dark blue here.	46
<u>Figure 19</u> Mean SODA current at 96m for period 1993-2005 at the Tristan da Cunha Archipelago with Etopo2 bathymetry as background, same as in Figure 18.	47
<u>Figure 20</u> Mean sub-surface SODA V-current component data in cm/s at 15°W for a) total water column, b) top 1000m and c) top 200m	48
<u>Figure 21</u> Normalised OISST anomaly at Gough Island 1982-2005	52
<u>Figure 22</u> Normalised OISST anomaly in °C at Tristan da Cunha Archipelago for January to May 1992. Tristan da Cunha (north) and Gough Island (south) are shown by white triangles.	52
<u>Figure 23</u> Air temperature (a) and precipitation (b) anomaly at Tristan da Cunha Archipelago for January to May 1992 obtained from the CDC website	53
<u>Figure 24</u> NCEP Mean wind (a) and anomaly for 1992 (b). Tristan da Cunha (north) and Gough Island (south) are shown by white triangles.	54
<u>Figure 25</u> NCEP anomaly for all El Niño years for wind (a) and Precipitation rate (b). Tristan da Cunha (north) and Gough Island (south) are shown by white triangles.	55

## 1.1 Introduction

From a physical Oceanographic perspective, the central South Atlantic is a sparsely studied region when compared to other Mid Ocean Basin regions (eg. Deacon, 1982; Stramma and Peterson, 1990; Lutjeharms *et al.*, 1993 and Smythe-Wright *et al.*, 1998). The central South Atlantic, the subtropical Indian Ocean, and the central South Pacific all have received little attention compared to the North Atlantic (Deacon, 1982). In depth biological (Barange *et al.*, 1998) and geological (Hofmann *et al.*, 2005) studies have been undertaken in the central South Atlantic, but with respect to the Subtropical Ocean Front, only a limited number of studies have been undertaken, and these are generally accepted as the norm. These include Deacon (1933), Stramma and Peterson (1990), Lutjeharms *et al.* (1993) and Smythe-Wright *et al.* (1998). The severe lack of long term meridional oceanographic transects in the South Atlantic make any attempt to define the basin-scale structure of ocean fronts futile. With the recent introduction of extensive global satellite derived sea surface temperature (SST) as well as sea level height (SLH) geostrophic current and wind products, new knowledge will be generated. However the need for in-situ ship-based observational datasets will never be reduced, as long as models do not represent real conditions. A major concern however, is the current inability to measure sea surface salinity from remote sensing, and the complex structure of ocean fronts that exhibit different surface and subsurface expressions (Lutjeharms *et al.*, 1993), could lead to biased positioning. This research will concentrate on the central South Atlantic in an attempt to more specifically identify the Subtropical Front (STF) in this region.

## 1.2 Subtropical Convergence/Front/Frontal Zone

### - 1.2.1 Discrepancy about use of term

In the South Atlantic, the region where warm Subtropical surface waters meet the cooler Subantarctic Surface waters is known as the Subtropical Convergence (STC) or the Subtropical Front (STF).

Krümmel (1882, as cited in Peterson *et al.*, 1996) was the first to notice this “sharp temperature discontinuity stretching across most of the South Atlantic” and named this temperature gradient the Subtropical Convergence. Since then, numerous authors (eg. Whitworth and Nowlin (1987) and Stramma and Peterson (1990)) have managed to change the common term given to this region to the Subtropical Front. It was argued that the general consensus within the scientific community was to reserve the term “Subtropical Convergence” for wind-driven surface convergence at 30° - 35°S, for which no evidence exists in the literature (Stramma and Peterson, 1990). The term “Subtropical Front” would be a better term for this oceanographic feature rather than “Subtropical Convergence”. Both terms are still generally accepted today, however the trend in recent years has been to use the former definition. Belkin and Gordon (1996) further characterized the region in the South Atlantic as having a northern and a southern branch, which they named the Northern Subtropical Front (NSTF) and the Southern Subtropical Front (SSTF). Collectively these fronts are regarded as the Subtropical Frontal Zone (STFZ). The argument to which term to use is evident in nearly every paper regarding this Subtropical Region. I have chosen to use Subtropical Front as the collective term for the temperature gradient as it is more in line with recent literature.

- 1.2.2 Criteria for surface STF identification

<b>Criteria for STF Identification</b>
Deacon (1933); Stramma and Peterson (1990); * Stramma (1992)
• Winter $T_0$ range = 11.5°-15.5°C
• Summer $T_0$ range = 14.5°-18.5°C
• Summer $S_0$ range at southern edge = 34.4 psu
Deacon (1937); Stramma and Peterson (1990); Stramma (1992)
<b>North of the STC</b>
• Winter $T_0$ range = 11.5°-16.5°C
• Summer $T_0$ range = 14.5°-19.5°C
• $S_0$ range = 34.9-35.5 psu
Deacon (1960)
• Winter $T_0$ range = 8°-12°C
• Summer $T_0$ range = 12°-16°C
Deacon (1982)
• $S_0$ range = 34.6-35.1 psu with axial $S_0 = 34.9$
* Burling (1961)
• Position of the 26.8 isopycnal at 200m
* Clifford (1983)
• Axial $T_{200} = 10^\circ\text{C}$ and axial $S_0 = 34.8$ psu
* Lutjeharms and Valentine (1984)
• $T_0$ range = 11°-18°C with axial $T_0 = 14.2^\circ\text{C}$
Whitworth and Nowlin (1987)
• $T_0$ range = 10°-14°C and axial $S_0 = 34.8$ psu
* Nagata <i>et al.</i> (1988)
• Axial $T_{150} = 12^\circ\text{C}$
* Orsi <i>et al.</i> (1993)
• Axial $T_{200} = 12^\circ\text{C}$
* Park <i>et al.</i> (1993)
• $T_{200}$ range = 8°-12°C with axial $T_{200} = 10^\circ\text{C}$
• $S_{200}$ range = 34.6-35.0 psu with axial $S_{200} = 34.8$
* Orsi <i>et al.</i> (1995)
• $T_{100}$ range 10°-12°C
• $S_{100}$ range 34.6-35.0 psu

*Table 1* Criteria for STF identification (adapted from Belkin and Gordon, 1996)

Please Note: References marked with a "\*" where taken from the review article Belkin and Gordon (1996)

Although a frontal zone is defined as a region of high horizontal gradients, which are either constant or varying over some depth interval, this study will focus primarily on the surface expression due to the use of mainly satellite SST datasets.

The definitions of the STF vary from author to author (Table 1). However from the table, one can deduce means of the axial (middle) values stated. Most definitions are ranges rather than singular values, which falls in line with Deacon's (1937) original proposition of a 4°C change in temperature and 0.5 psu change in salinity. Different ranges of values for isotherms also exist for the different seasons. No actual values have thus far been assigned for the surface identification of the STF, other than mean values for the ranges.

In the following study a combination of all the ranges were chosen in Table 1. Using the range of Lutjeharms and Valentine (1984) as the parent range due to its wide scope, 11°C to 18°C, and slightly adjusting for the outlying 10°C isotherm in Whitworth and Nowlin's (1987) range, resultant values of 18°C and 10°C for the extreme northern and southern boundary of the STF arise. The mean value of 14.2°C of Lutjeharms and Valentine (1984) was selected. In this manner all suggested surface criteria in Table 1 were represented.

### 1.3 General circulation of the South Atlantic,

#### - 1.3.1 STF in the South Atlantic

As long ago as the early 19<sup>th</sup> century, it was known that a persistent eastward drift existed in the central South Atlantic, and was running east or east-northeast from Tristan da Cunha. The first to attempt to describe this South Atlantic circulation was Major Rennel in 1832 (as cited in Peterson *et al.*, 1996). He described this drift as the

Southern Connecting Current, stating that it ran along 39°S and even postulating that the westerly wind belt might be the driving force. Captain Beaufort attempted to then trace it across the South Atlantic from west to east but only managed to do so up to 22°W before losing it. Major Rennel (1832, as cited in Peterson *et al.*, 1996) was also first to correctly describe the circulation of the east coast of Brazil and cited the confluence, situated between 30° and 40°S to be the source of the STF. For many years Major Rennel's description of the South Atlantic was widely accepted by the scientific community, and little further effort was put into refining the research. The majority of the research at this time was concentrated at the edges of the South Atlantic. Only in 1882 did Otto Krümmel (as cited in Peterson *et al.*, 1996) undertake a basin scale description of the STF, from its formation at the Brazil/Malvinas Confluence across to as far as Gough Island at 40.5°S and 9°W, describing its path as "a sharp temperature contrast".

In the 20<sup>th</sup> century, most of the research undertaken, used Deacon's (1933) definition of 4-5°C Temperature change and 0.5psu change in Salinity, when describing the STF. 20<sup>th</sup> century researchers also defined it as the boundary between the Subtropical gyre and the Antarctic Circumpolar Current (ACC), and stated that whilst in the long term, the STF may be described as a zone of convergence, in the short term it exhibits a much more complex nature (Campos *et al.*, 1999).

The majority of the literature, with regards to the formation and general position of the STF across the South Atlantic, stems from investigations done by Stramma and Peterson (1990), Peterson and Stramma (1991) and Smythe-Wright *et al.* (1998). The following study will mostly concentrate on their work, as it is relevant to the central South Atlantic.

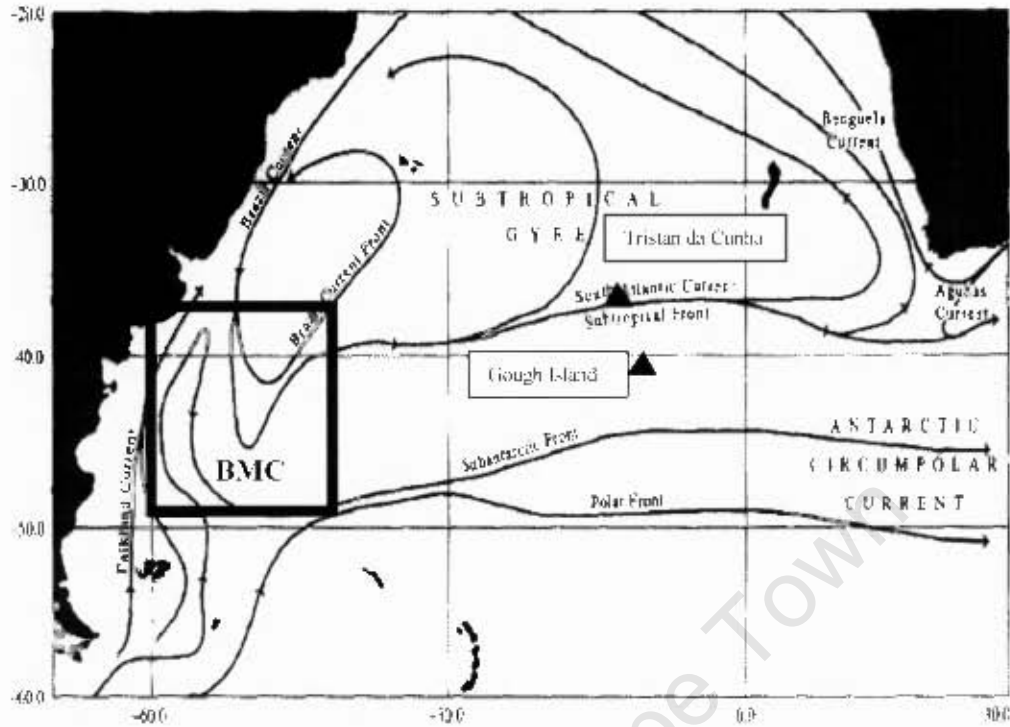


*Figure 1* The position of the fronts and large-scale circulation in the South Atlantic Ocean (Smythe-Wright *et al.*, 1998), with the Tristan Archipelago and the Brazil/Malvinas Confluence (BMC) identified.

The STF is not part of the circumpolar current as there are no subtropical waters found in the Drake Passage, (Stramma and Peterson, 1990). This implies a formation off the east coast of Brazil and it is assumed therefore, that the source of the STF is within the Brazil/Malvinas Confluence (BMC) Zone (enclosed area in Figure 1). Cold sub Antarctic waters that are advected northward by the Falklands Current, meet the warm waters from the Brazil Current and are forced offshore at a latitude of 42°S. This offshore movement was described by Peterson and Stramma (1991) as being both the STF and Brazil Current Front. The two frontal features are difficult to distinguish from one another due to both having similar salinities and that the

resulting gradients are weak. From there, the STF undertakes an organisational phase to approximately 45°W in an intense eddy field such that Roden (1986) found the two features distinguishable from one another between 40° and 42°W. The Brazil Current then branches off to the north to re-circulate with the waters in the Argentine Basin. The STF can still exhibit great positional variation at this longitude, with meanders as far south as 46°S having been recorded between 55° and 40°W (Stramma and Peterson, 1990).

In the central South Atlantic, Belkin and Gordon (1996) divide the STF into a northern and a southern branch, the NSTF and the SSTF. They defined the frontal zone to be up to 5° latitude wide and stated then, that it could exhibit properties of several temperature gradients bounded by regions of homogenous waters. Earlier work suggested that the structure and location of the STF to the west of Greenwich is uncertain (Shannon *et al.*, 1989). Peterson and Stramma (1991) gave a general position of 2° to 3° north of 40°S. However, further eastward, at the 0° meridian, the STF moves south of 40°S, mainly due to the forcing by the Agulhas Retroflexion region (Smythe-Wright *et al.*, 1998; Belkin and Gordon, 1996). Both Deacon (1982) and Peterson and Stramma (1991) attributed this southward shift to bathymetric forcing of the continental shelf.

The main driving mechanism behind the STF/SAC at the southern boundary of the subtropical gyre is the prevailing westerly winds. According to the Sverdrup theory, subtropical gyres are driven by wind curl due to the transition from tropical trade winds, to the high latitudes westerlies.



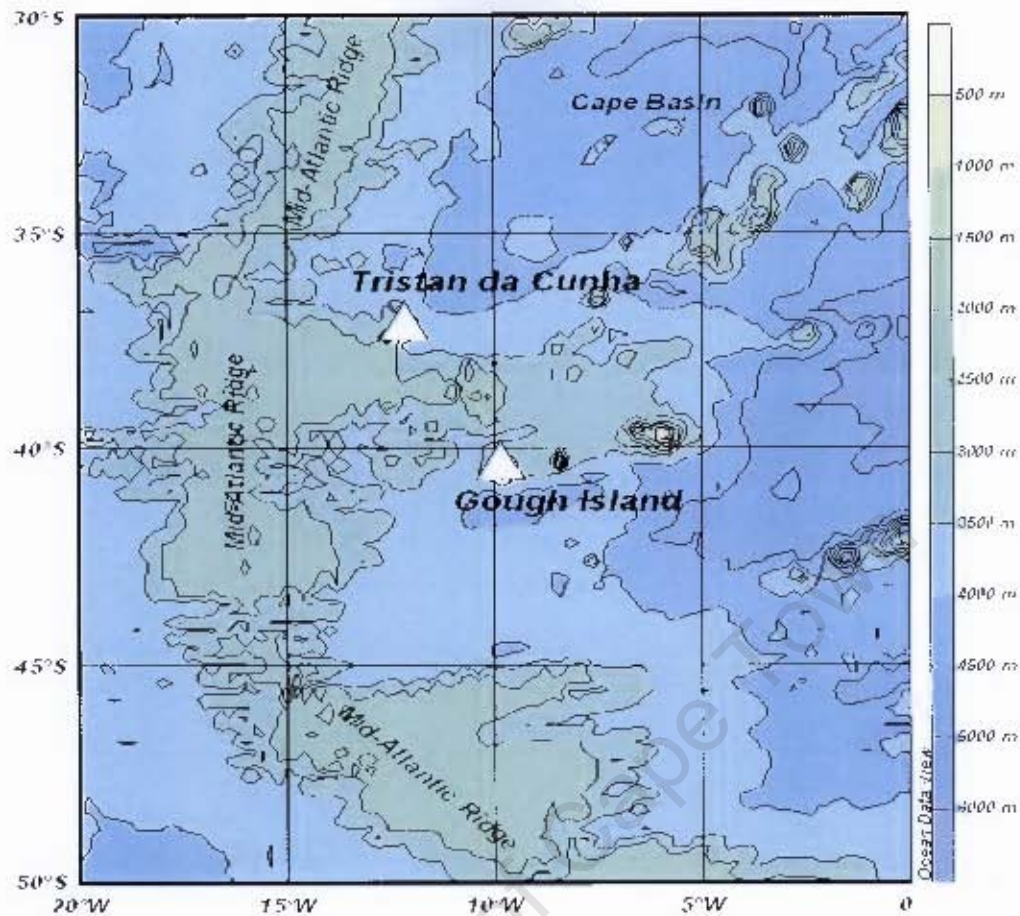


*Figure 2* The Region of Interest centred on the Tristan da Cunha Archipelago, hereafter depicted as white triangles, showing their location to the east of the prominent Mid-Atlantic Ridge.

### 1.3.2 The South Atlantic Current

At the southern limit of the subtropical gyre, where the STF borders the ACC, Stramma and Peterson (1990) reported on the South Atlantic Current (SAC) that is said to flow along the northern border of the STF (Figure 1 at Tristan da Cunha). They also stated that the SAC is not coupled to the STF as they followed different tracks at 42-43°W and that the SAC does not flow into the South Indian Ocean while

the STF does. Smythe-Wright *et al.* (1998) defined the SAC to rather be bound between the NSTF and the SSTF. Stramma and Peterson (1990) also concluded that due to the lack of hydrographic datasets in the central South Atlantic, it would be impossible to investigate what effects the mid-ocean ridge might have on the SAC transport. Smythe-Wright *et al.* (1998) refuted Stramma and Peterson's (1990) theory of slowing down of the SAC at the mid-ocean ridge, rather attributing this to re-circulation of subtropical waters into the Argentine Basin west of 20°W (Refer to Figure 1, Page 6). They further stated that the SAC flows primarily in the upper 1000m, which strengthens Stramma and England's (1999) statement that there is no depth dependent shift in the central region. The transport of South Atlantic Central Water (SACW) by the SAC in the central region was said to be in the order of 15 Sv (Stramma and Peterson, 1990), 11-28 Sv (Smythe-Wright *et al.*, 1998), and 9-12 Sv (Mercier *et al.*, 2003). Of this transport, some flows into the Indian Ocean while some contributes to the Benguela Current and the rest re-circulates (Stramma and England, 1999). Surface speeds of the SAC range from Whitworth and Nowlin's (1987) estimate of 13cm/s relative to the bottom at the Greenwich meridian, to Roden's (1986) calculated 20-26 cm/s.

#### 1.4 Previous studies in the central South Atlantic region

##### - 1.4.1 Physical oceanographic studies

The majority of the research undertaken in the South Atlantic has been constrained to the borders of the Subtropical gyre, close to the continents on either side. Most of the literature concentrates on cruises done in the 1980s and 1990s (Smythe-Wright *et al.*, 1998) and contains a high degree of interpolation. During the late 20<sup>th</sup> and early 21<sup>st</sup>

century, the use of satellite datasets for tracking the surface expression was increasingly used (Lutjeharms *et al.*, 1993; Burls and Reason, 2006).

Small-scale research close to Gough Island, where 32 stations were occupied, was undertaken during austral spring of 1980. The temperature and salinity results have shown that the waters were essentially of sub-Antarctic origin, implying that the STF was to the north of Gough Island at the time (Miller and Tromp, 1982). Knox (1960, as cited in Andrew *et al.*, 1995) believed the STF to be situated to the north of Gough Island in summer and to the north of Tristan da Cunha in winter. Miller and Tromp (1982) also postulated that the water characteristics could be influenced by the position of the STF and that there could be topographical effects from the island itself, such as a baroclinic eddy downstream of the island, which could cause vertical upwelling.

Over a period of 17 months, from October 1988 to March 1990, SST and salinity measurements were undertaken at Tristan da Cunha. The results revealed that during the sampling period, the Tristan da Cunha Island Group always lay within the STFZ, although from the sea surface salinity samples one could not infer latitudinal changes of the STF (Andrew *et al.*, 1995). Temperature readings showed a 4°C range from 15° to 19°C in summer and a 2°C range from 13° to 15°C in winter. The temperatures at Gough were roughly 3°C lower on average. Andrew *et al.* (1995) hypothesised that the apparent southward shift of the STF across the island was not due to an overflow of warmer waters but rather due to insolation during summer months, based on observed salinity measurements. The increased stratification would in turn increase the primary production in the south.

The South-east Atlantic Expedition in austral autumn of 1989 had numerous aims, in anticipation of the World Ocean Circulation Experiment (WOCE), one of which, was to document the position and structure of the STF to the west of the Greenwich meridian, and to possibly use satellites for future investigation (Shannon *et al.*, 1989). During the expedition, the STF at 13°W was found to not be a single front but rather to exhibit a multiple frontal structure. Its location was found to be centred between 37° and 38°S. This discovery was to be more common in later years.

Peterson and Stramma (1991) stated that the STF lies, for the most part, 2-3° north of 40°S, while closer to the continents it could be found further south. The authors assigned a value of 11.5°C and 14.5°C for the winter and summer minimum SST respectively (Stramma and Peterson, 1990).

Belkin and Gordon (1996) argued that the front described by Deacon (1937) was in actual fact the SSTF, and that he never found the NSTF. Deacon (1937) also stated that the STF was variable by up to 600km or 6° latitude but attributed this to unusual large-scale movements related to meteorological changes (Smythe-Wright *et al.*, 1998). Belkin and Gordon (1996) also stated that the NSTF and SSTF are distinguishable features across the South Atlantic, from the east coast of Brazil to the Benguela region off the South African west coast. A similar Frontal Zone is found in the South Pacific (Belkin and Gordon, 1996) and Indian Ocean south of Australia (Sokolov and Rintoul, 2002). The theory of a frontal zone rather than a single front was consistent with previous results.

Smythe-Wright *et al.* (1998) used a collection of cruise data to attempt to characterise the STF in the central South Atlantic. The data included the South-east Atlantic Expedition of Shannon *et al.* (1989), the WOCE A11 line in 1993, the SAVE leg 4 in 1989, the SAVE leg 5 in 1989, the Ajax leg 1 in 1983 and the V2 line in 1978. They concluded that the NSTF varied by 1.5° latitude and the SSTF by up to 2.5° latitude. They postulated that SSTF remains to the south of Tristan da Cunha and gave mean values of 18.6°C and 35.5 psu for the NSTF and 14.9°C and 34.9 psu for the SSTF.

- 1.4.2 Central South Atlantic – Geological and Biological oceanographic studies

A study to identify the position of the STF during interglacial periods was undertaken by Hofmann *et al.* (2005), by measuring the lithologic variations from cores taken across the STF in the Southern Atlantic Ocean. The merging of Sub Antarctic Surface Water (SASW) from the south with Antarctic Intermediate water (AAIW) after subducting under the SACW from the north, and the associated deep water masses comprising of nutrient poor North Atlantic Deep Water (NADW) and nutrient rich Antarctic Bottom Water (AABW), all contribute strongly to affect the sediment accumulation rates and composition (Hofmann *et al.*, 2005). Taking cores from this region, the authors concluded that during the Quaternary Period, the STF had a tendency to exhibit temporal shifts. Berger and Wefer (1996, as cited in Hofmann *et al.*, 2005) postulated a northward shift of the STF during glacial periods, which could be inferred from the results of Hofmann *et al.* (2005) as the cores taken from the northward side of the STF exhibited properties of the STF currently lying to the south.

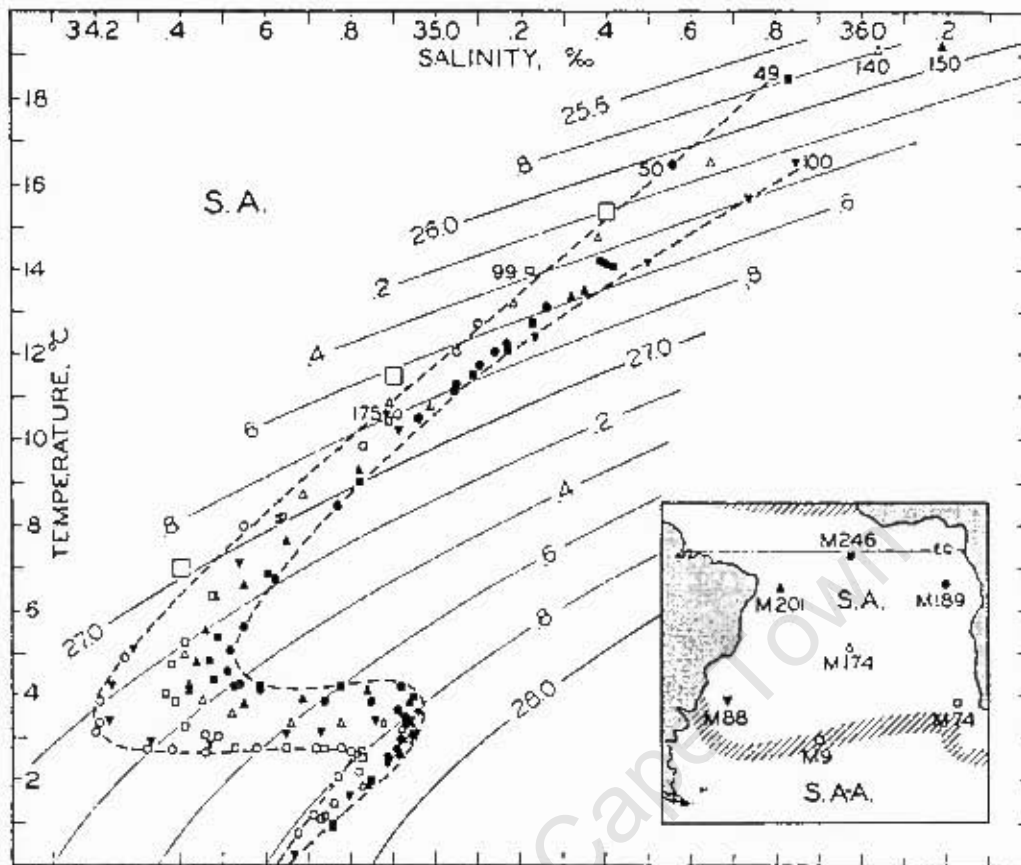


*Figure 3* Temperature-Salinity diagram for the waters present in the South Atlantic Ocean. The shaded region depicts the possible location of the STF (From Sverdrup *et al.*, 1942)

It has been documented that the STF may also act as biogeographic boundary for phytoplankton, zooplankton, cephalopods, fish and even birds (Deacon, 1982; Lutjeharms and Valentine, 1987; Andrew *et al.*, 1995; Froneman *et al.*, 1997; Barange *et al.*, 1998; Cuthbert *et al.*, 2005). Mackintosh (1960) stated that the STF was the southern boundary of warm water planktonic species, implying that species were linked to specific water masses (as cited in Deacon, 1982).

Biological sampling was also undertaken in the region of interest. Andrew *et al.* (1995) attempted to classify fish catches. They concluded that the fish fauna was inherently different at Tristan da Cunha and Gough Island, as only 3-4 of the epipelagic species found at Tristan da Cunha, could also be found at Gough Island. Of the 28 neritic species known for the region of interest, 26 were found at Tristan da Cunha and only 19 at Gough Island. Of the 51 species during the survey, 21 were present exclusively to the north of the STF.

Barange *et al.* (1998) work in the South Atlantic was located more to the east, with sampling stations near 3°E and 19°E. Their results showed that there should be difference in dynamics between the western location and the location south of Africa, due to the structure of the fish fauna. The position of the STF at 3°E was found to be highly variable and temporary, as it did not maintain its characteristics for more than 2 to 3 weeks (Barange *et al.*, 1998). They attributed this transient nature to the lack of interaction with western boundary currents, as the thermal gradient was more intense closer to the African continent where more observations had been recorded. Here, the increase in biomass lead to pelagic production and cross-frontal mixing, as they found species of subtropical and Antarctic origin on both sides of the front (Barange *et al.*, 1998). The fish structure present in the interior of the STFZ was dominated by species distinctive of intermediary fauna.

The distribution of micro-phytoplankton in the STFZ showed highest concentrations at the southern boundary and at the periphery of a warm core eddy. Froneman *et al.* (1997) highlighted the importance of eddies shed off from the Agulhas retroflection region, as a mechanism for transport of micro-phytoplankton across the STF.

Tracked Albatrosses in the South Atlantic were found to exclusively remain in the region 50°W to 15°E and 30-45°S as they are attracted to biological “hotspots” rich in nutrients (Cuthbert *et al.*, 2005).

The northern region above the STF was nutrient poor with strong vertical stratification as opposed to the southern region, which had high concentration of nutrients but weak stratification (Llido *et al.*, 2005). From satellite data, regions along the STF showed periods of enhanced chlorophyll-*a* concentrations along a region of high mesoscale turbulence (Weeks and Shillington, 1996). Llido *et al.* (2005) used SeaWiifs satellite chlorophyll-*a* data, along with a three-dimensional model, to investigate the forcing of bloom events at the STF to the south of Africa. They deduced that cloudless, calm conditions caused a chlorophyll bloom during spring 1998.

#### - 1.4.3 Central South Atlantic – Satellite derived oceanographic studies

Satellite data have increasingly been used to study remote regions not continuously accessible by ship. One of the first published reports on the surface expression of the STF in the central South Atlantic from satellite data was done by Lutjeharms *et al.* (1993). They defined the front to be ‘ephemeral’, a term used by numerous authors since to describe the temporal latitudinal variation of the front. Lutjeharms *et al.* (1993) also stated that the STF is better defined as a salinity front rather than a thermal one, as the surface and subsurface expression may not correspond. Earlier work by Lutjeharms and Valentine (1987) suggested that the STF was not only a surface feature as was evident to up to 1000m depth. Lutjeharms *et al.* (1993) used



data from a cruise along the Greenwich Meridian from October 1983 to January 1984, which showed the STF to be situated at 37°S. More cruise data from an oblique crossing during December 1989 to January 1990 showed a strong salinity gradient at 43°S to the west of Tristan da Cunha. A further front at 38°S and another at 34°S was also found. According to Lutjeharms *et al.*, (1993) the southern most front was in actual fact still part of the STFZ, whereas Gordon *et al.* (1992, as cited in Lutjeharms *et al.*, 1993) termed this to be the Sub Antarctic Front (SAF). They also highlighted the difference in expressed position from the South-east Atlantic Expedition in austral autumn of 1989. The salinity gradient showed the STF to be situated at 37°S but the thermal front was expressed at approximately 40°S. Satellite data suggest that the most latitudinal variability is in the region of the mid-ocean ridge (Lutjeharms *et al.*, 1993).

An intensive study on SST fronts in the central South Atlantic from microwave-sensed data was undertaken by Burls and Reason (2006). Their work refutes previous studies suggesting that the STF existed as a continuous band across the South Atlantic in terms of SST. Tracking meridional gradients rather than surface isotherms, they identified multiple fronts within the STFZ creating a complex zone. The gradients ranged between 0.015 and 0.025°C/km. A strong surface gradient was observed throughout the year at 45°S, but this was associated with the SAF. The strength and latitudinal location of the STF was shown to have pronounced variability on an interannual timescale. Causes of this may be due to the shifts in wind and thus the meridional position of the strongest wind stress curl, as the affect could only be seen at the surface, not below the mixed layer (Burls and Reason, 2006).

At the eastern and western border of the subtropical gyre however their findings were consistent with previous studies. To the east of  $15^{\circ}\text{W}$ , the STF could be defined as the NSTF and the SSTF. Strengthening of these fronts was observed during austral spring and winter along with a slight shift in position (Burls and Reason, 2006).

From the Greenwich meridian to the Agulhas Retroflection region, Burls and Reason (2006) identified pronounced mesoscale variability. The variation was rather caused by frontal intensity than by the shifting of the strong gradients in this region.

Lutjeharms and Valentine (1987) assumed that shifts and meanders resulting from extensive eddy shedding at the Agulhas Retroflection region could cause some of the variability.

This chapter highlights that a poor understanding exists along with insufficient data on the seasonality of the STF. As new model datasets are increasingly used to overcome the data shortfall, these still need to be challenged with actual measured data to confirm their validity.

## 1.5 Study Aims

This research project aims to investigate the following in the central South Atlantic

- Can we ascertain the seasonality of the STF from OISST and AMSR data?

To date the exact movement of the STF past the Tristan da Cunha Archipelago has not been properly defined. Using the 24yr OISST dataset as well as the higher resolution AMSR-E dataset of 2002-2006, an attempt is made to better describe the movement. This will be done using a revised definition for the surface identification of the STF as that previously described in Table 1.

- AVISO geostrophic currents in the central South Atlantic and comparison to SODA

The use of oceanographic model datasets are more prevalent in recent times to alleviate the shortcomings of actual in-situ data. To investigate the validity of SODA model dataset in the central South Atlantic it is compared with AVISO satellite derived geostrophic currents. The model simulation is also used to investigate the potential effect of bathymetric forcing on the currents surrounding the Tristan da Cunha Archipelago.

- Origin of a cold event

Anomalous SST events at the Tristan da Cunha Archipelago could have an adverse affect on the fishing industry, on which the livelihood of the inhabitants is heavily dependent. A cold event is defined and studied in the region surrounding the Tristan da Cunha Archipelago in the central South Atlantic. The possible forcing of this event is investigated using the Climate Diagnostic Center website ([www.cdc.noaa.gov](http://www.cdc.noaa.gov)).

The mid-South Atlantic and the Tristan da Cunha Archipelago is one of the least understood areas from an oceanographic perspective, due to its isolated location and very few continuous datasets have been collected in this area (Refer to Figure 4 and Table 2). The only continuous dataset comes from the South African operated meteorological station situated on Gough Island at approximately 40°S and 9°W, which collects SST, SLP, wind readings and precipitation data. The majority of oceanographic cruises in the area collected data only during austral summer, which makes defining the longitudinal variation and seasonal changes impossible (Lutjeharms *et al.*, 1993). Lutjeharms and Valentine (1987) also questioned the validity of the XBT data that had mostly been collected during austral summer, saying that such data could be seasonally biased. With latitudinal variations of 6° documented (Deacon, 1937), and the recent introduction of continuous satellite datasets easily accessible on the Internet, a wider range of research, with respect to the STF in the central South Atlantic, has been introduced (Burls and Reason, 2006). Furthermore, various other data can be inferred from a single type of satellite measurement. Satellite SST measurements have the potential to be used to infer fronts as well as eddies (Rouault and Lutjeharms, 2003) and ocean currents (Isern-Fontanet *et al.*, 2006).

Although Argo floats have been operational worldwide since 2003, their data are omitted as the focus is more on the surface expression of the STF in the South Atlantic rather than the more stable subsurface expression.

Also the NOAA operated WOCE line AX18 data were omitted due to them being mainly zonal in extent and would so not adequately display latitudinal variation

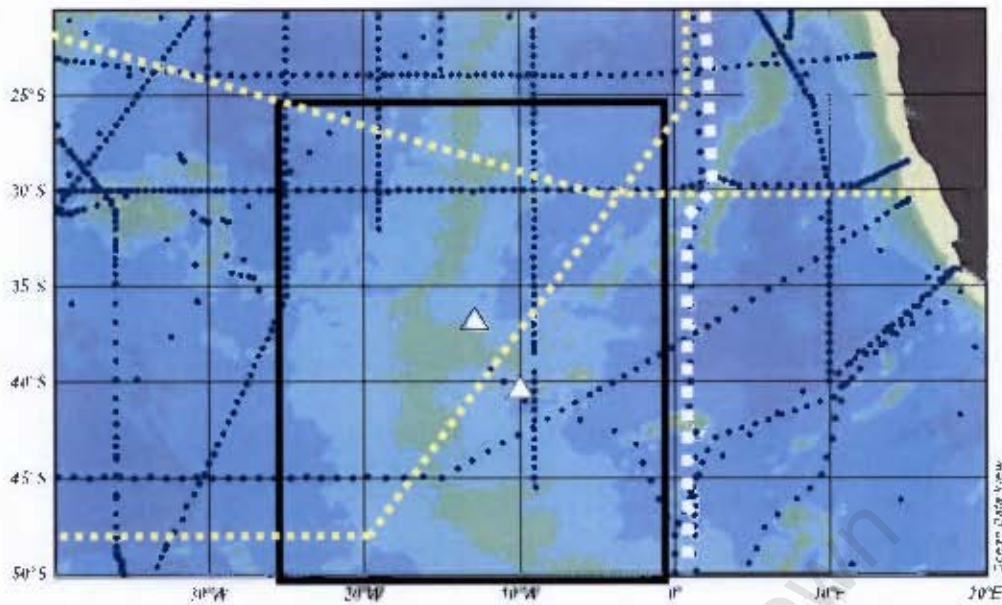


*Figure 4* Compilation of World Ocean Circulation Experiment (WOCE, blue) lines, South Atlantic Ventilation Experiment (SAVE, yellow) lines and the Ajax leg 1 (white) line in the South Atlantic available in the WOCE and SAVE database at the end of the 20<sup>th</sup> century highlighting the sparseness of data in the Region of Interest (represented by the enclosed area). Tristan da Cunha (north) and Gough Island (south) are shown by white triangles.

Line	R/V Name	Year
WOCE A10	<u>Meteor</u>	1992/1993
WOCE A11	<u>Discovery</u>	1992/1993
WOCE A13	<u>L'Atalante</u>	1995
WOCE A14	<u>L'Atalante</u>	1995
WOCE A16C	<u>Melville</u>	1989
WOCE A16N	<u>Oceanus</u>	1988
WOCE A16S	<u>Melville</u>	1989
SAVE Leg 3	<u>Knorr</u>	1988
SAVE Leg 4	<u>Melville</u>	1988
Ajax leg 1	<u>Knorr</u>	1983

*Table 2* Details for WOCE and SAVE lines within the enclosed area in Figure 4 above

## 2.1 Data sources and characteristics

### - 2.1.1 Gough Island in-situ SST data

Historical SST data from the Meteorological station on Gough Island was received from the South African Weather Bureau (SAWB) in daily format and manually transferred into a computer. The data extend from 1956 to 2005 to make a comprehensive 50 year time series. The original daily datum was averaged into monthly means over each month, and gaps filled using the GISST interpolated dataset of Melice *et al.* (2003).

### - 2.1.2 NOAA OISST v.2 data

Monthly Optimally Interpolated Sea Surface Temperature (OISST) version 2 data were extracted from the National Ocean and Atmosphere Administration (NOAA) website ([www.cdc.noaa.gov](http://www.cdc.noaa.gov)) for the period extending from January 1982 to December 2005 resulting in 24 years of extensive coverage. The data were adjusted to only cover the area from 19.5°S to 60°S and from 35°W to 10°E, so that it centred on the Tristan da Cunha Archipelago.

OISST v.2 dataset is a 1-degree resolution dataset produced weekly from analysis in-situ and satellite SST data as well as SST's simulated by sea-ice cover (Reynolds *et al.*, 2002). Satellite bias is removed before analysis as described in Reynolds (1988). The data are screened according to the reliability of the source. The satellite data are compared to in situ ship and drifting buoy data. Outliers occur due to several reasons, mainly because the algorithms used for SST determination fail (Reynolds, 1988).

Other reasons include difference between day and night time algorithms, cloud top interference and the presence of aerosols in the atmosphere due to volcanoes.

Averaging daily values linearly interpolated from the weekly dataset over a month creates monthly OISST v.2 data.

### - 2.1.3 AMSR-E SST data

Monthly SST data from the area surrounding the Tristan da Cunha archipelago were obtained from Advanced Microwave Scanning Radiometer (AMSR-E) instrument on NASA's Aqua spacecraft, downloaded from the Remote Sensing Systems (REMSS) website ([www.remss.com](http://www.remss.com)). The extracted domain extends from  $-30^{\circ}\text{S}$  to  $-50^{\circ}\text{S}$  and from  $25^{\circ}\text{W}$  to the Greenwich meridian for the years 2003 to 2006.

It measures SST at a  $\frac{1}{4}^{\circ}$  spatial resolution. Monthly composites are computed by taking the average of all the data within one calendar month. Its' most important asset over previously launched SST measuring systems, is that microwave observations have the ability to not be affected by cloud cover, enabling scientists to receive uninterrupted data of SST. Until recently microwave observations have been too coarse resolution (Rouault and Lutjeharms, 2003) to be of use. Due to its short orbiting period up to now, only 4 years worth of data have been collected. This may result in some bias with respect to both average and anomaly calculations.

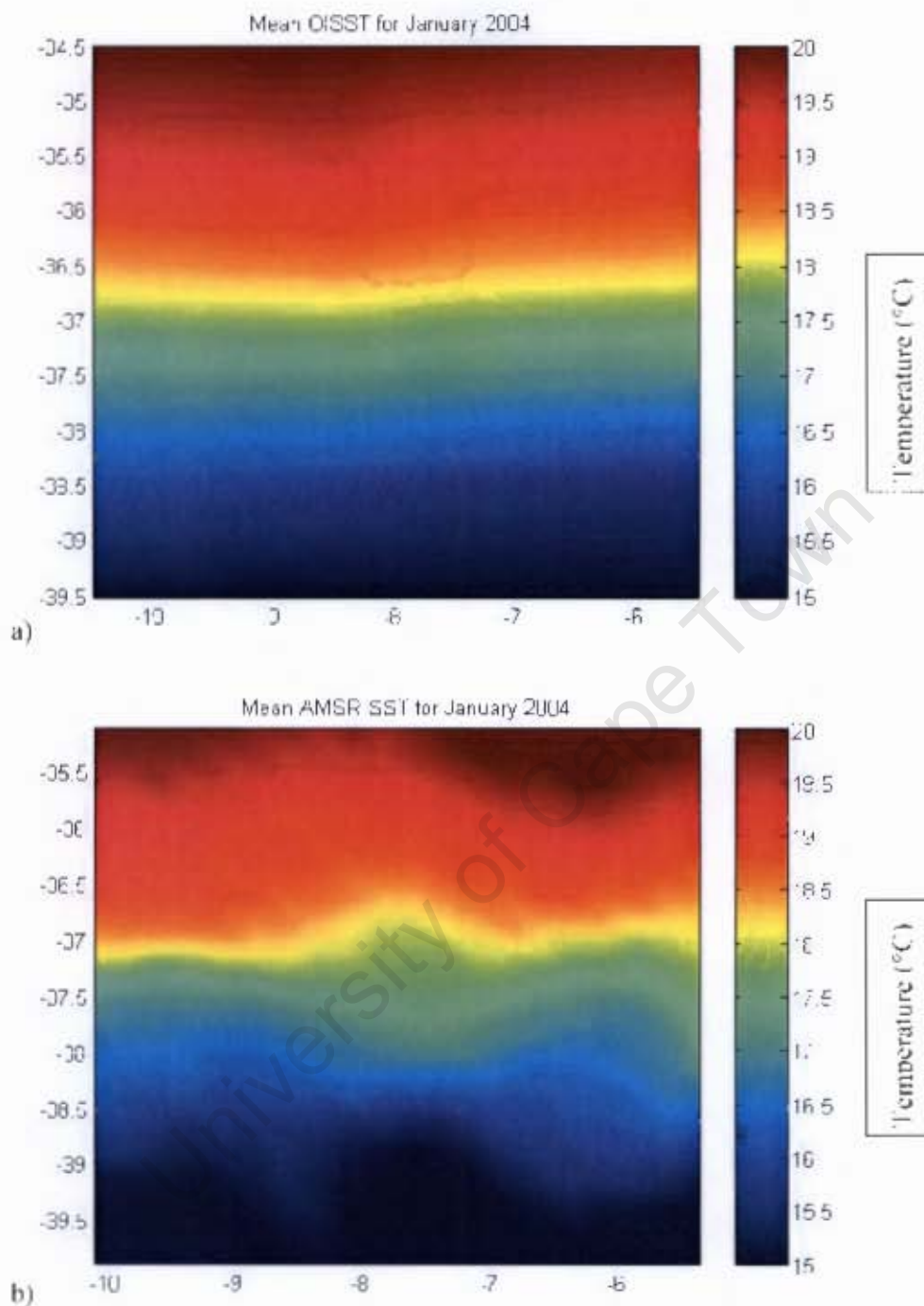


*Figure 5* Mean SST in °C for OISST data (a) and AMSR data (b) for January 2004 in a region downstream of Tristan da Cunha, highlighting the higher spatial resolution of the AMSR dataset over the OISST dataset, which has the higher temporal resolution.



Emery *et al.* (2006) found AMSR SST data have a high correlation ( $r > 0.99$ ) with in-situ, thermal infrared and ARGO float profiling data in the Labrador Sea. Its accuracy in our region of interest can therefore not be severely questioned.

- 2.1.4 AVISO geostrophic current data

The AVISO (Archiving, Validation and Interpretation of Satellite Oceanographic data) altimetry derived geostrophic current data are constructed using delayed-time merged altimetry satellite data from the Topex/Poseidon, Jason-1, ERS-1 and ERS-2, and EnviSat satellites and the data are available from the AVISO website (<http://las.aviso.oceanobs.com>). Altimetry uses the Doris precise orbit determination and positioning, to accurately determine the precise location of the aforementioned satellites. These, in turn, measure their height above the sea surface using radar. The SSH is then estimated by calculating the difference between the satellite height and the altimetric range. This value takes into account the difference in sea level due to gravitational variations, known as the geoid, as well as the dynamic topography due to ocean circulation. From SSH then one can infer ocean currents through geostrophy, where the slope on the sea surface is directly related to the pressure gradient. A balance between the horizontal pressure gradient and the Coriolis force results in a flow along the lines of equal rate of change. A deflection “down slope” in the southern hemisphere is to the left.

#### - 2.1.5 SODA model data

Simple Ocean Data Assimilation (SODA) is a reanalysis product of an ocean model with actual observations. The gridded dataset attempts to simulate the World's oceans as accurately as possible. SODA was created by Carton *et al.*, (2000a) at the Department of Atmospheric and Ocean Science at the University of Maryland. Forcing of the SODA 1.2 model is done by ERA-40 winds. Later model runs include subsurface temperature and salinity data that come from existing World Ocean Database 2001, which have already undergone strict quality control and make up approximately two-thirds of the dataset. The altimeter data come from AVISO and the NASA Pathfinder Program in the later models.

Data were extracted from the website

<http://iridl.ldeo.columbia.edu/SOURCES/CARTON-GIESE/SODA/v1p4p2/> as

monthly means starting January 1958 and ending December 2001, making a total of 528 months, or 44 years. Each month contained temperature, salinity, current (u and v component) and sea surface height, and covered an area from 25°S to 50°S and 30°W to Greenwich. In this region, the depth-associated variables were divided into 34 subsurface levels, ranging from 5 meters at the surface to 3874m near the bottom. The first 9 levels make up the top 96m while the next 13 levels cover 112m-918m, finally, the last 12 levels are in intervals of roughly 250m. SSH was only present on the surface. The spatial resolution is  $\frac{1}{2}^\circ$ .

- 2.1.6 Etopo2 bathymetry data

Etopo2v2 bathymetry dataset is a 2-minute latitude/longitude gridded seafloor and land elevation dataset obtained from U.S. Department of Commerce, National Oceanic and Atmospheric Administration, National Geophysical Data Center, 2006 (<http://www.ngdc.noaa.gov/mgg/fliers/06mvg01.html>). A combination of satellite altimetry readings, shipboard echo-sounding measurements, and data from the Digital Bathymetric Data Base Variable Resolution are the main contributors to the Etopo2v2 dataset.

- 2.1.7 Live Access Server (LAS) Websites

NCEP/NCAR reanalysis climate data were used to investigate circulation anomalies over an extended region across the islands. These were computed using monthly and seasonal climate composites obtained from the Climate Diagnostic Center website ([www.cdc.noaa.gov](http://www.cdc.noaa.gov), August 2007). In isolation, this data should be treated cautiously due to lack of observations, particularly south of 40°S prior to 1970 (Rouault *et al.*, 2005), however since comparisons are made with respect to recent data, this caution is not applicable.

## 2.2 Methodology

- 2.2.1. Calculations of associated means, anomalies
- 2.2.1.1. Monthly, yearly and overall means

All datasets, irrespective of their original form, were averaged into monthly means for their period of coverage in order to make comparison between the datasets possible.

This was done using the “mean” and “nanmean” functions available in MatLab v.6.5.

The “mean” function is represented by equation (1).

$$(1) \quad mean = \frac{\sum_{i=1}^n x_i}{n}$$

Daily data, like those in the Gough Island SST dataset, were averaged over the month by adding up all data points and dividing the total by the number of days in that month. Missing data were subtracted from the number of days for that month to still give monthly mean using the “nanmean” function, which simply ignores missing values. These missing data were then smoothed out using a three-month running mean over the 50 years, similar to that used by Melice *et al.* (2003) using the “smooth” (equation (2)) function in MatLab v.6.5.

$$(2) \quad smooth = \frac{[x_{i-1} + x_i + x_{i+1}]}{3}$$

OISST, AMSR and SODA data were already available as monthly mean data and needed no further manipulation to get them into the required format.

AVISO data are available in weekly mean format, which are 5-day means over the duration of the data available. No monthly means were computed as only the 13 year

mean was used. The Yearly mean was simply computed by averaging all the yearly data.

- 2.2.1.2. Anomaly and normalised anomaly calculations

To calculate anomalies from the data, the overall mean was first calculated as described in 2.2.1.1. This value was then subtracted from each data point to give the anomaly as a deviation from the aforementioned mean.

Normalised anomaly was calculated using the “norm” function in MatLab v.6.5. The “norm” function (equation (3)) first subtracts the mean from the anomaly, and then divides this value by the standard deviation to get a value as a standard deviation from

0. (3) 
$$norm = \frac{x_i - mean}{stddev}$$

- 2.2.1.3. Latitudinal temperature gradients in °C/km

MatLab v.6.5 was again used for calculating the latitudinal temperature gradients using the “gradient” function (equation (4)). This resulted in a rate of change per latitudinal data point (°C/data point). Then, using the “deg2km” function, the total distance in km was calculated and then divided by the number of data points to get a value of km/data point (equation (5)). The rate of change per latitudinal data point (°C/data point, equation (4)) was then divided by km/data point (equation (5)) to get a value of °C/km .

(4) 
$$LatTgrad = \frac{\partial Temperature}{\partial Latitude}$$

(5) 
$$Equl = \frac{deg\ 2km(\partial Latitude)}{n}$$

## - Chapter 3 RESULTS

### 3.1 Introduction to Region of Interest

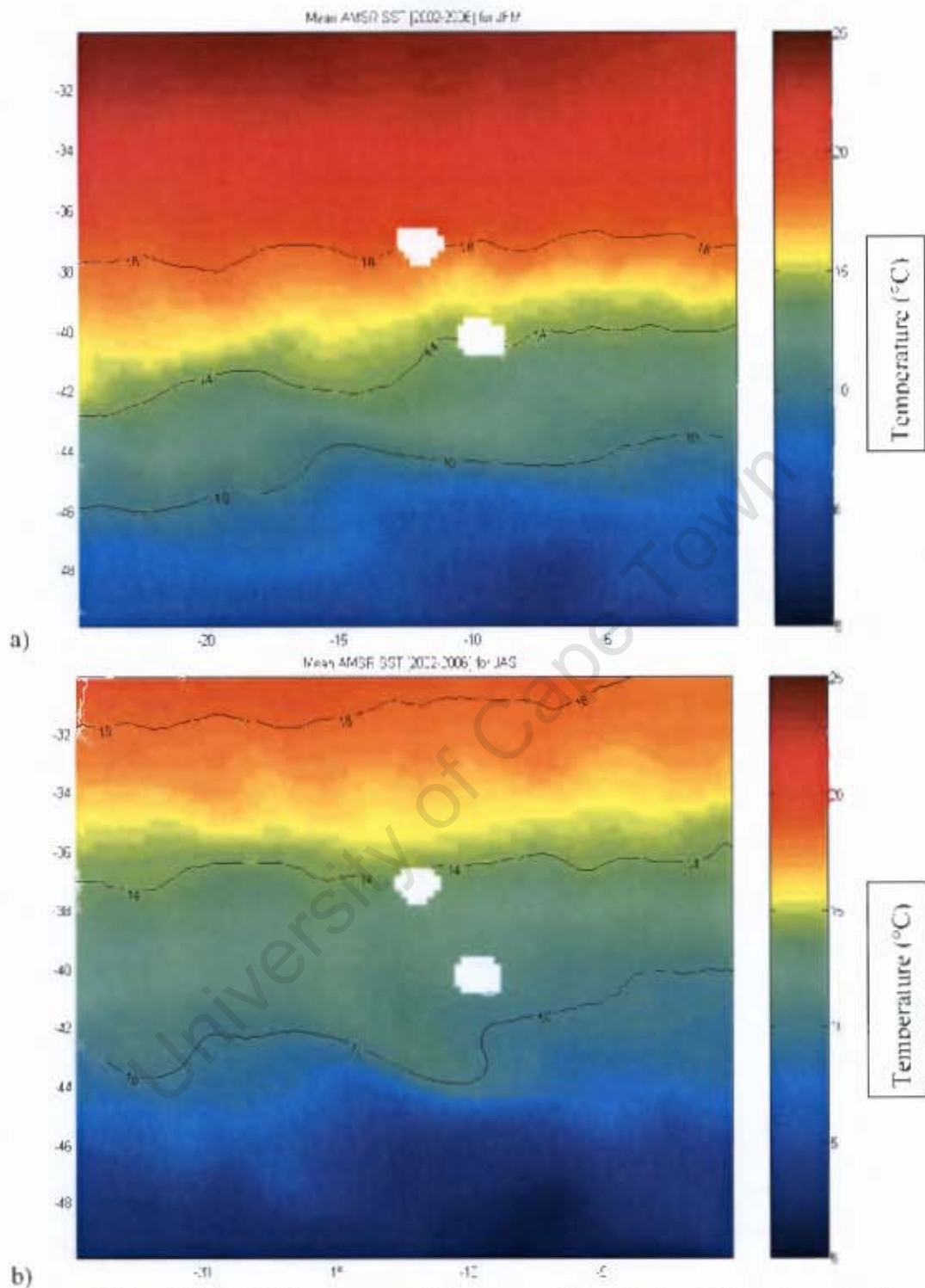
A relative sparseness of hydrographic data exists in the central South Atlantic which is only now being overcome with the use of new satellite derived data.

On a smaller scale, the aim of this work is to concentrate on the region of the Tristan da Cunha archipelago. The Archipelago consists of Tristan da Cunha Island, situated at 37°S 12°W, Nightingale and Inaccessible Islands, approximately 20 nautical miles to the south west, and Gough Island, which lies 230 nautical miles to the south east of Tristan da Cunha. The region of interest covers an area from approximately 25°S to 50°S, and 25°W to the Greenwich meridian. Some datasets used will have slightly different coordinates for clarity, but they are all centred round the archipelago.

#### - 3.1.1. Mean SST

Mean SST for the region of interest is shown in Figure 6 using Microwave SST of 30km resolution, which has the ability to collect SST in the presence of clouds.

Collective means of the summer (January, February and March) and winter (July, August and September) months show that the three depicted isotherms (10°C, 14°C and 18°C) have a latitudinal variation of approximately 4°. The 14°C isotherm does not exhibit latitudinal movement further south than Gough Island in summer, and further north than Tristan da Cunha in winter. The 10°C isotherm remains fairly constant in the region 15°-10°W at approximately 44°S.



**a)**  
**b)**  
**Figure 6** Mean SST in °C for January, February and March (a) and July, August and September (b) from AMSR SST data for the period 2002-2006. The data are described in Chapter 2. The white areas are Tristan da Cunha (north) and Gough Island (south).

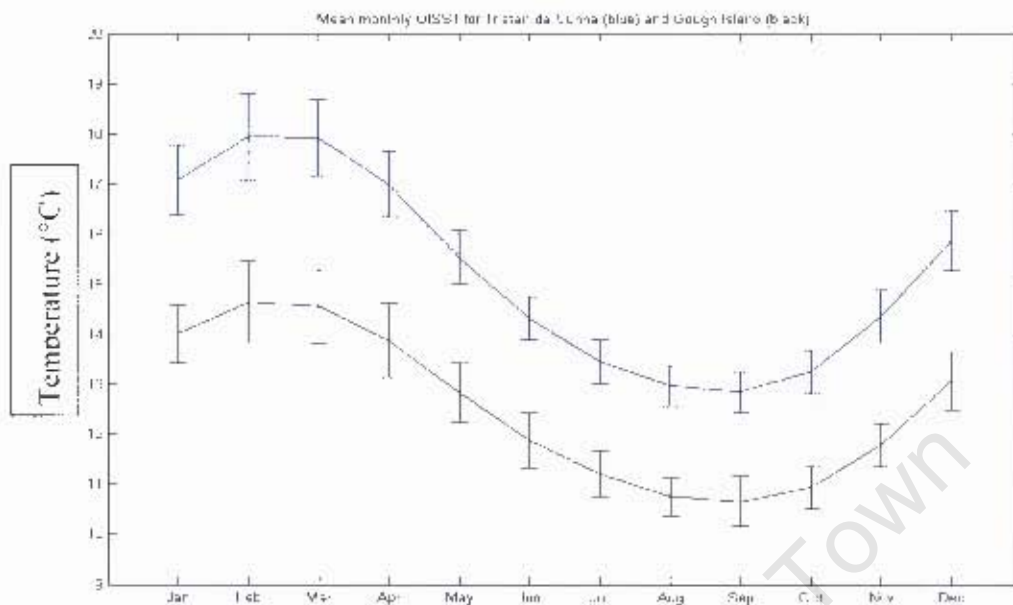


*Figure 7* Mean monthly SST in °C for Tristan da Cunha (blue) and Gough Island (black) from 24 years of OISST data with bars depicting standard deviations.

Optimally Interpolated Sea Surface Temperature (OISST, see chapter 2 for explanation) derived means for Tristan da Cunha and Gough Island are represented in Figure 7. Due to the short duration of AMSR data I used OISST to depict the seasonal cycle. The maximum temperature at Tristan da Cunha occurs in the late summer months of February and March, reaching nearly 18°C. The lowest recorded mean water temperatures are present approximately 6 months later, during August and September, with temperatures in the region of 13°C. This agrees with Smythe-Wright *et al.* (1998) who stated it was obvious from the data that the warmer (colder) period would fall under late summer (winter) months in the central South Atlantic. Gough Island exhibits a very similar trend with warm SST during February and cold SST during September. These however are approximately 3°C colder than temperatures at Tristan da Cunha and confirms the study of Andrew *et al.* (1995). The summer



months are shown to have a larger variability than the winter months. Both Tristan da Cunha and Gough Island have a standard deviation of  $\pm 0.8^{\circ}\text{C}$  during February and  $\pm 0.4^{\circ}\text{C}$  during August.

- 3.1.2. Mean sub-surface temperature, salinity and U-current component

Previous studies in the Southern Ocean have confidently compared SODA with hydrographic data, highlighting the usefulness of SODA as an investigative tool (*pers.comm.* Ansorge).

A 44 year mean of sub-surface SODA reanalysed temperature data at  $15^{\circ}\text{W}$  reveals a fairly uniform appearance north of  $40^{\circ}\text{S}$  with a temperature change with increasing depths of approximately  $4^{\circ}\text{C}$  per 100m, and isotherms inclined southwards (Figure 8). This suggests that there is significant mixing of the surface waters, as was seen by Miller and Tromp (1982) at latitude corresponding to Gough Island. South of  $40^{\circ}\text{S}$  however the isotherm inclination increases sharply, that at  $44^{\circ}\text{S}$  the  $4^{\circ}\text{C}$  isotherm rises from a depth of 800m to less than 100m over a latitudinal distance of  $2^{\circ}$ . Using the different definitions from Table 1 the STF lies between  $40^{\circ}\text{S}$  and  $44^{\circ}\text{S}$  from the subsurface expression, which would not be largely different from the surface expression. As mentioned earlier, it needs to be stressed though that the surface and subsurface expression can differ substantially (Lutjeharms *et al.*, 1993; Barange *et al.*, 1998). The surface expression is situated predominantly to the south of the subsurface expression at approximately  $42^{\circ}\text{S}$ , and is less pronounced over a larger area in the central South Atlantic than to the south of Africa (Barange *et al.*, 1998).

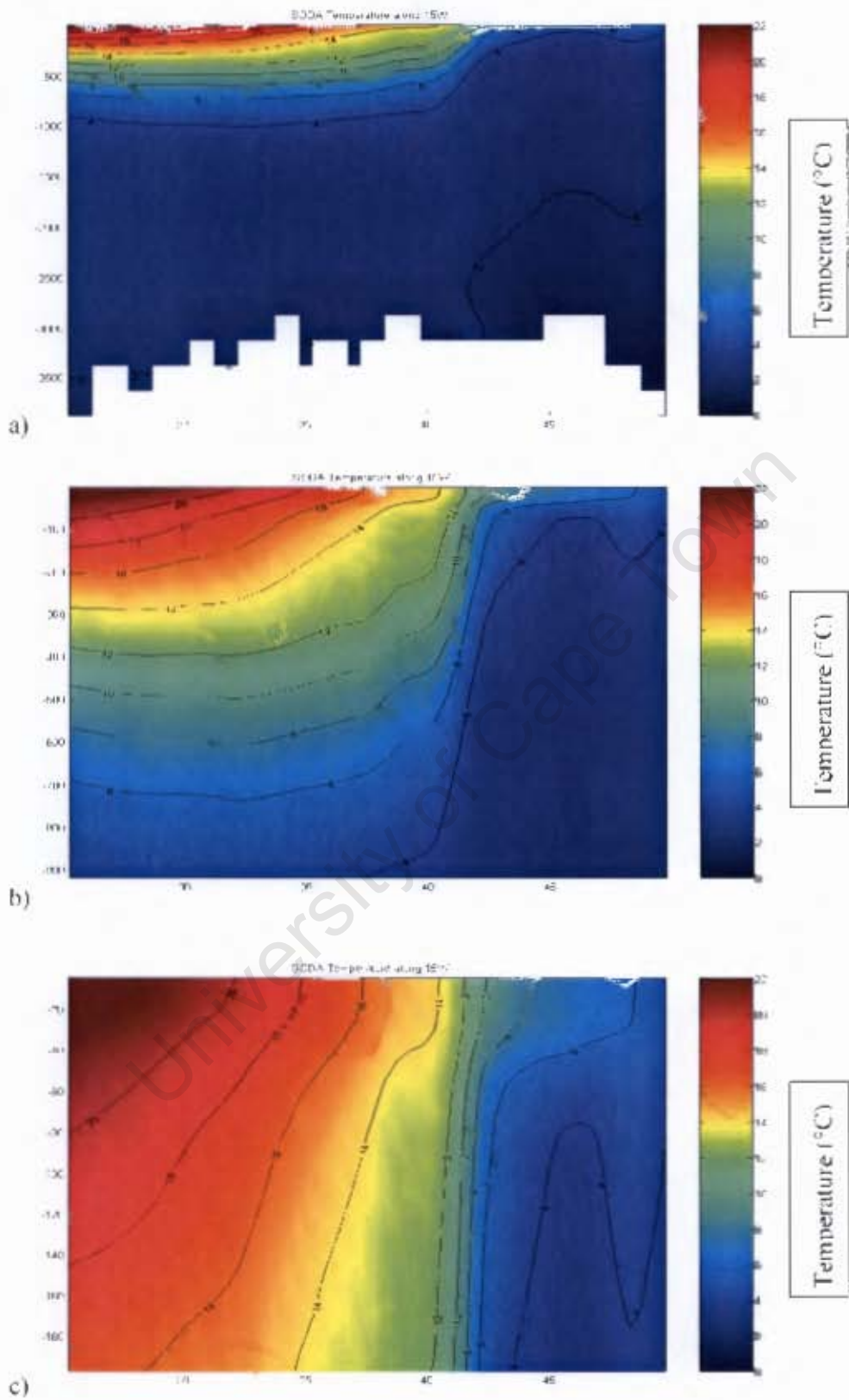


*Figure 8* Mean sub-surface SODA temperature data in °C at 15°W for a) total water column, b) top 1000m and c) top 200m

Lutjeharms *et al.* (1993) stated that identification of the STF would be more reliable by using salinity as the proxy. This is however not yet possible with satellite remote sensing, so the SODA reanalysed salinity dataset is used. As before, using the criteria from Table 1, the STF can be defined from the mean transect at 15°W in Figure 9 as being situated approximately between 38°S and 42°S, depending which definition one uses. Using the axial value of 34.9 psu, the STF lies at 41°S, based on the mean. A subsurface salinity maximum as described by Smythe-Wright *et al.* (1998) is clearly visible (Figure 9b). This is said to be formed at the NSTF by a convective process of cooling and sinking (Smythe-Wright *et al.*, 1998).

Using the same transect to show the U-current component (Figure 10), it becomes evident that the SODA model portrays a strong east-ward current with values exceeding 35cm/s in the region centred at 42°S. This coincides with the strong surface temperature gradient associated steeply inclined isotherms (Figure 8) and shoaling of isohalines (Figure 9).

A much weaker east-ward current is evident at 47°S with a speed just exceeding 5cm/s.

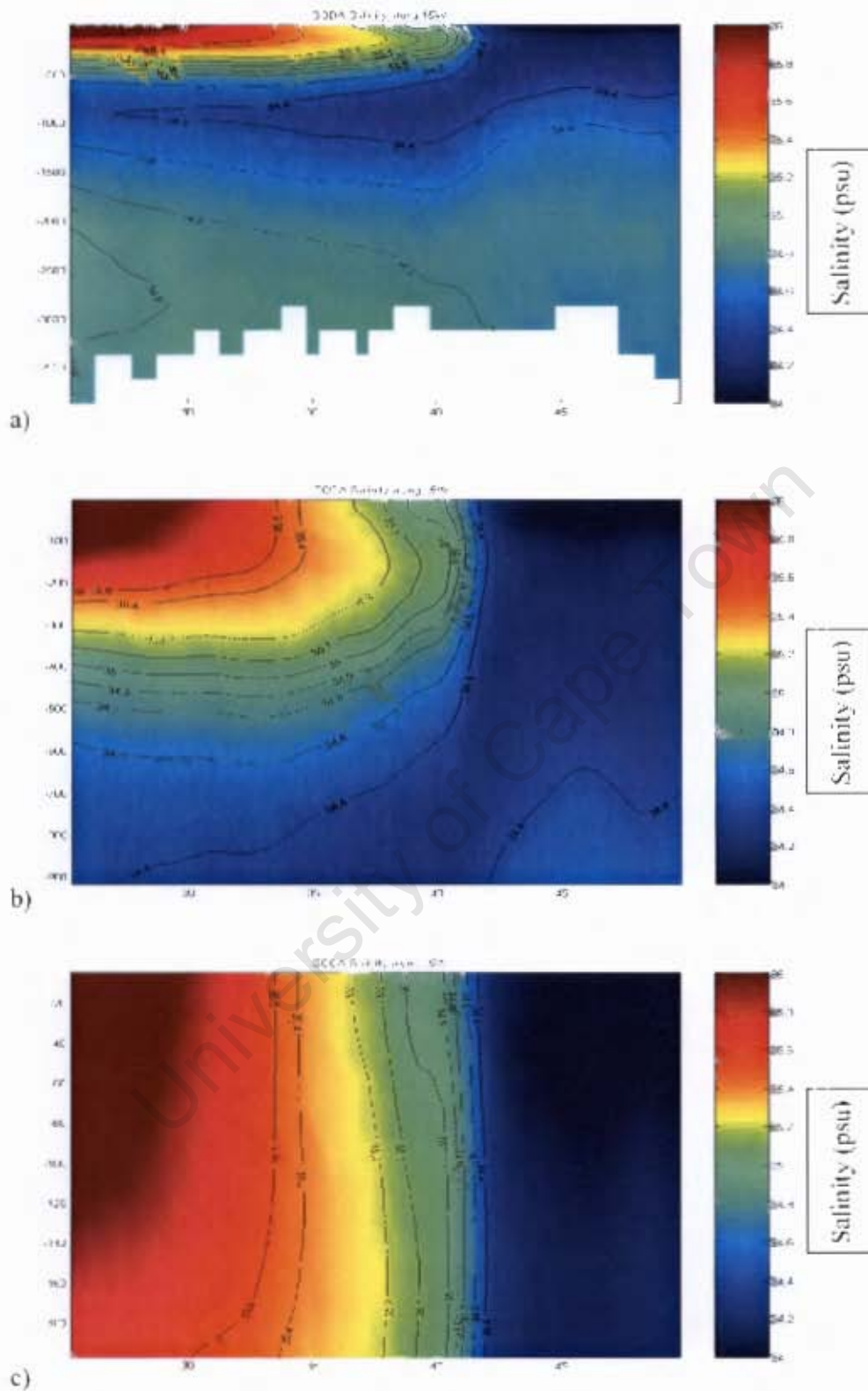


*Figure 9* Mean sub-surface SODA salinity data in psu at 15°W a) total water column, b) top 1000m and c) top 200m

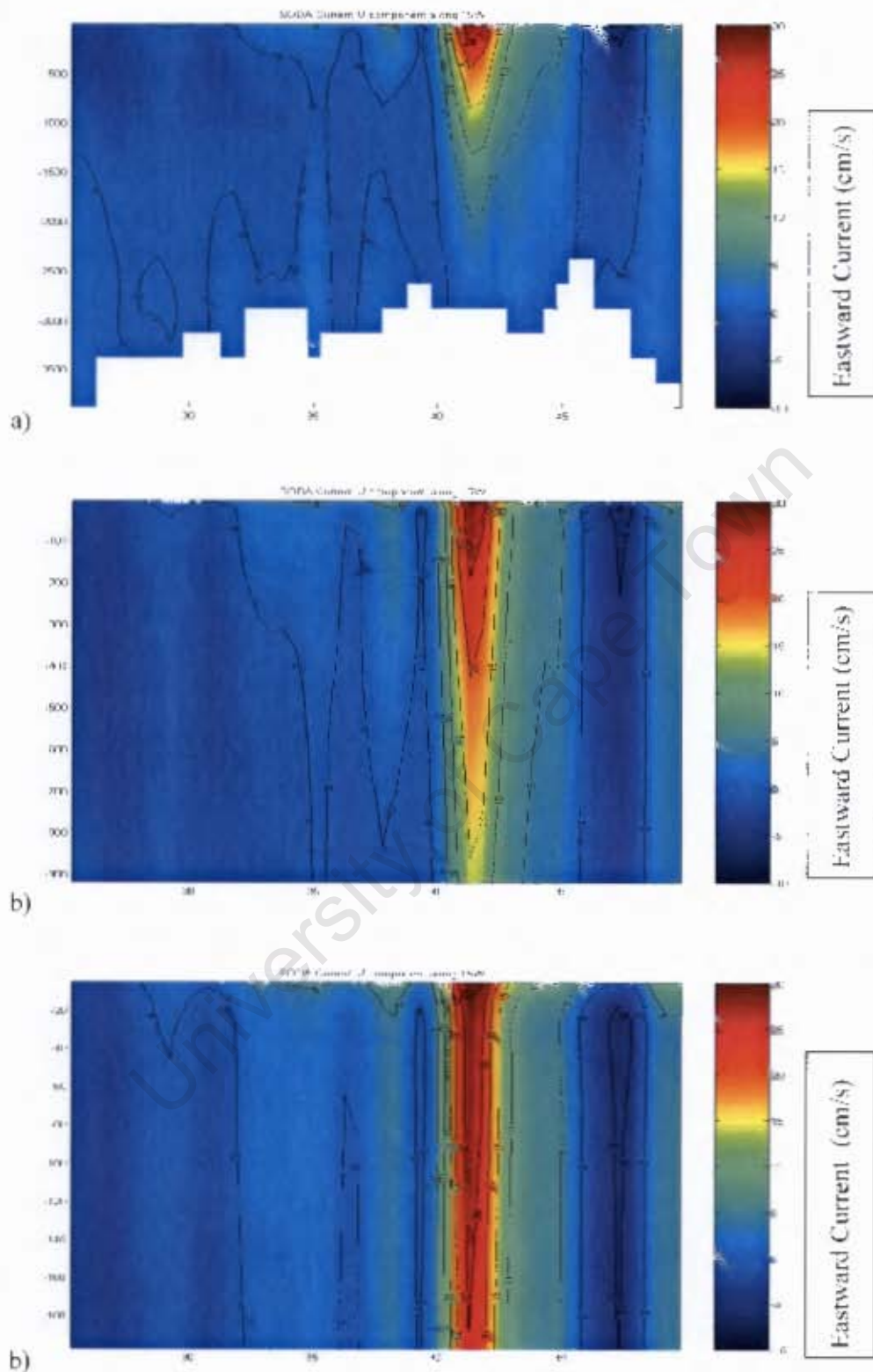


*Figure 10* Mean sub-surface SODA U-current component data in m/s at 15°W for a) total water column, b) top 1000m and c) top 200m

### - 3.1.3. Mean circulations

To study the circulation the absolute geostrophic current were used, presented in Figure 11. Not much seasonal variation exists between summer and winter mean currents for the region of interest, as is shown in Figure 11. The most prominent feature is the region of strong current, extending from 15°W to 5°W and from 42°S to 46°S. Burls and Reason (2006) noted that this region had a temperature gradient of 0.04°C/km and strengthened significantly in the winter months and could be attributed to the Sub Antarctic Front (SAF). Further north, along 35°S, the SAC has an organised structure up to 15°W with core surface speeds of over 10cm/s before branching into various minor structures with associated speeds of 8cm/s or less in the vicinity of Tristan da Cunha. Along approximately 18°S lies the Atlantic South Equatorial Current flowing at a rate of 8cm/s.

The mean currents at Tristan da Cunha and Gough Island (Figure 12) show that although the two islands are only 430km apart, they experience different strengths and directions of currents throughout the year. During all months except June, the current flows from the southwest at Tristan da Cunha, increasing during summer with speeds of over 10cm/s. A weak westerly current component is present during early to middle winter. Gough Island experiences southwesterly currents only during the second half of the year with maximum speeds of 5cm/s. From late summer though to austral autumn a westerly current dominates, before turning back to southwesterly again during May.

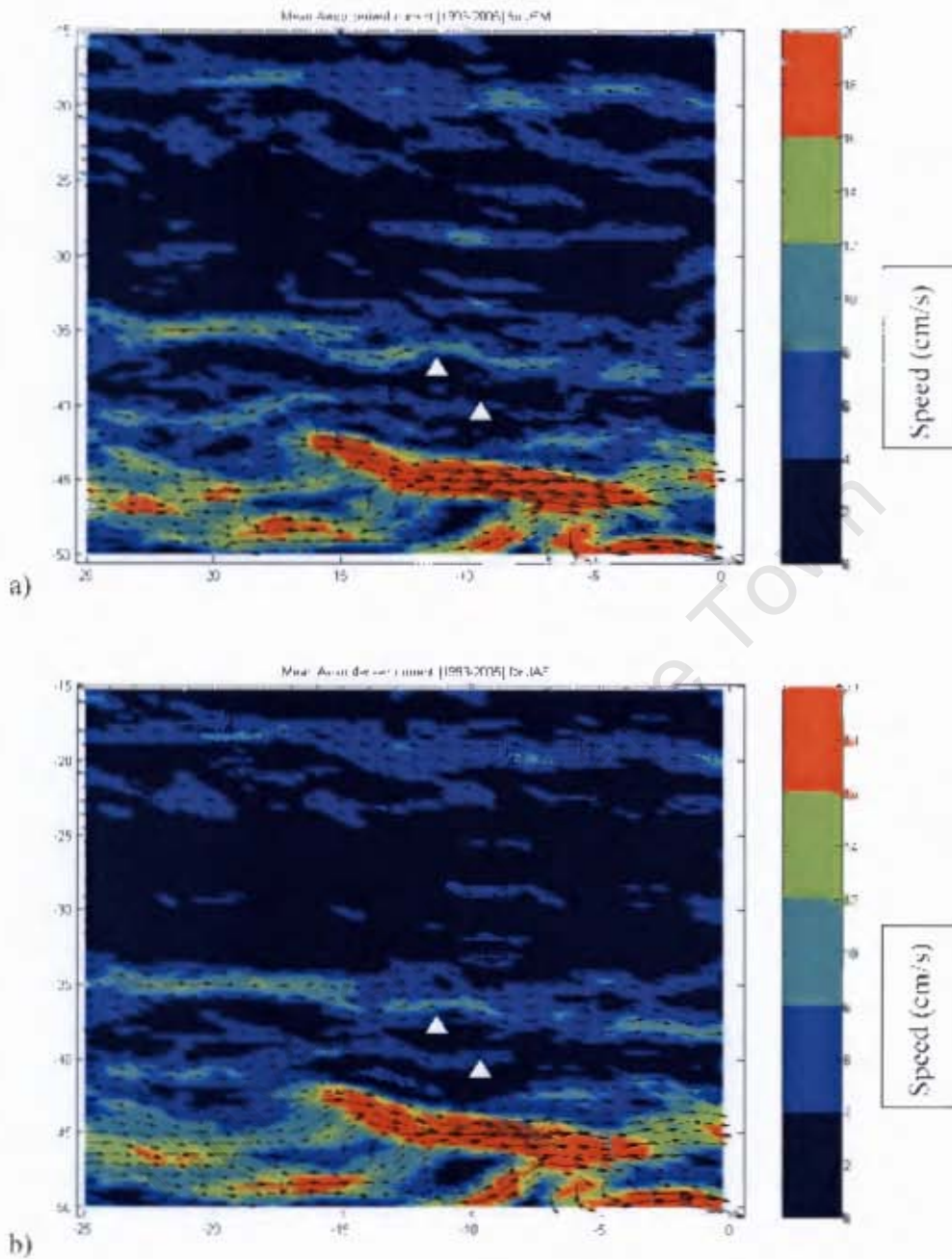


*Figure 11* Mean AVISO absolute geostrophic current in cm/s for January, February and March (a) and July, August and September (b), highlighting the broad zone difference of current strength in the region.

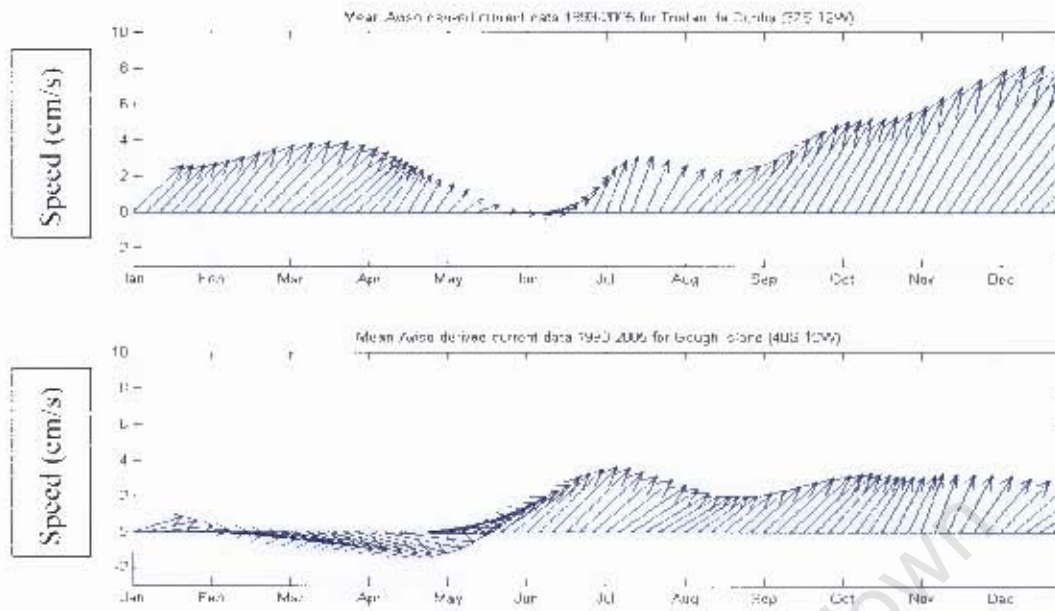


*Figure 12* Mean AVISO absolute geostrophic current in cm/s for points situated at Tristan da Cunha (top) and Gough Island (bottom)

The remote location of the region of interest results in a relative sparseness of in-situ oceanographic data. With the improvements in satellite derived oceanographic data and computer generated ocean simulations in recent times, the severe lack of data in this region is overcome. These data are compared to in-situ data to increase the scope at which the region can be viewed, as well as testing its credibility in a comparison with what is already known.

### 3.2 Can we ascertain the seasonality of the STF from OISST and AMSR data?

Gough Island SST data have been collected for the past 50 years. These are compared in Figure 13 to OISST data for the period 1982 to 2005. The data evident in Figure 13a were found to have a correlation coefficient of 0,90 at the 95% confidence interval. The biggest differences are in March 1985, when OISST is 2.08°C warmer,



and in May 1995, when Gough Island SST is 2.04°C warmer. When seasonal means are compared, the OISST dataset is, on average, 0.28°C warmer. The largest difference is during February, with that month being 0.53°C warmer. The smallest difference is during early summer, when November is only 0.17°C warmer.

Because of the 90% correlation between OISST and in-situ Gough Island SST data, one can confidently use the OISST data as being representative of the oceanographic environment in the central South Atlantic, keeping in mind that the OISST would be consistently higher.

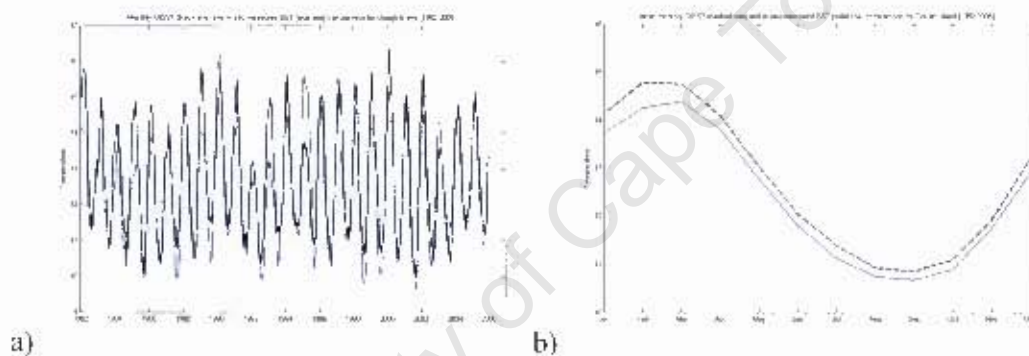


*Figure 13* OISST comparison with in-situ Gough Island SST for 1982-2005 (a) and seasonal mean (b)

The 11°W meridian was used in order to find a median value for the Tristan da Cunha archipelago, as it lies just between Tristan da Cunha and Gough Island.

As mentioned earlier in Chapter 1.2, no definite singular value has been assigned in the literature to the STF in the central South Atlantic, but rather a 4°C temperature range. Using values obtained from Table 1 it was decided to use a combination of assigned values. Lutjeharms and Valentine's (1984) range of 11°C to 18°C and the axial value of 14.2°C was the main one used. This was however slightly adjusted in the colder domain to 10°C to accommodate for Whitworth and Nowlin's (1987) range

of 10°C to 14°C. The resultant isotherms of 18°C and 10°C for the northern and southern boundary respectively with a median value of 14.2°C were chosen. This was done to encompass nearly all ranges found in Table 1. Figure 14 shows a Hovmöller plot at 11°W from 24 years of OISST data to highlight the inter-seasonal changes in this region. The movement of the possible surface expression of the STF, as well as other oceanographic features, can be traced over a period dating back 24 years at 11°W. Using a latitudinal temperature gradient one can identify a region of near constant rate of change of 0.012°C/km, situated between the 18°C and the 14.2°C isotherm. Although the OISST data have been proven to be consistently warmer throughout the season, one can still take the results to be true as the rate of change would still be the same.

At 42°S to 46°S there is a region with values consistently higher than 0.014°C/km, as was found by Burls and Reason (2006).

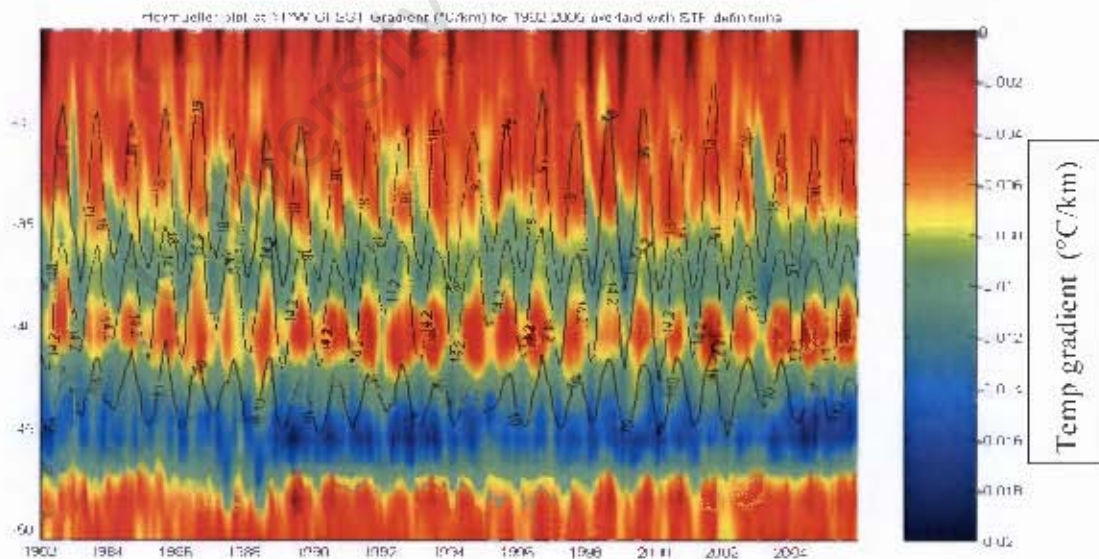


*Figure 14* Hovmöller plot of OISST latitudinal temperature gradient for 1982 to 2005 overlaid with isotherms assigned to STF temperature ranges, highlighting the stable seasonal signal

When one uses a higher resolution dataset such as AMSR satellite SST as shown in Figure 15, which has a  $\frac{1}{4}^\circ$  resolution compared to the  $1^\circ$  resolution of OISST, then the results are slightly different. The constant rate of change of  $0.012^\circ\text{C}/\text{km}$  is still slightly evident between the  $18^\circ\text{C}$  and the  $14.2^\circ\text{C}$  isotherm, but can go as high as  $0.02^\circ\text{C}/\text{km}$ . The region at  $42^\circ\text{S}$  to  $46^\circ\text{S}$  shows more intense values than in the OISST data, going beyond  $0.02^\circ\text{C}/\text{km}$ . The region at  $42^\circ\text{S}$  shows the lowest rate of change, remaining between  $0^\circ\text{C}$  and  $0.002^\circ\text{C}/\text{km}$ , exhibiting near latitudinal homogenous characteristics.

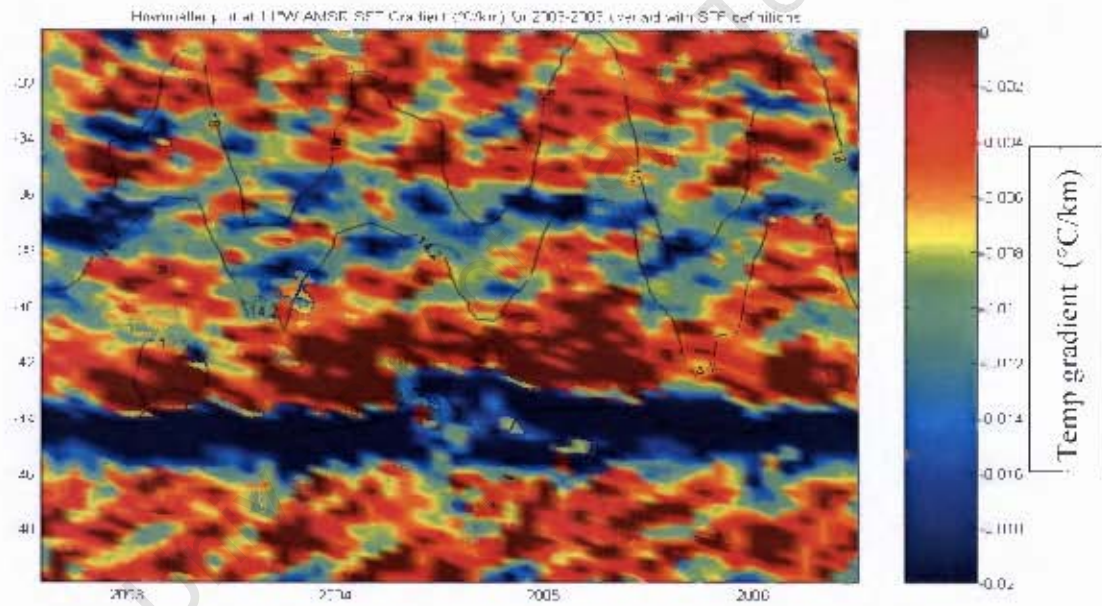


*Figure 15* Hovmöller plot of AMSR latitudinal temperature gradient for 2003 to 2006 overlaid with isotherms assigned to STF temperature ranges

Using the  $0.012^\circ\text{C}/\text{km}$  gradient as the indicator for the STFZ, one can deduce that the front has maximum latitudinal variation between  $34^\circ$  and  $41^\circ\text{S}$  at  $11^\circ\text{W}$ . During an average year, the location would be between  $36^\circ$  and  $39^\circ\text{S}$ , with summer months between  $37^\circ$  and  $40^\circ\text{S}$  and winter months between  $36^\circ$  and  $38^\circ\text{S}$ .

A mean of the latitudinal temperature gradient over the whole region of interest (Figure 16) shows the near constant rate of change of  $0.012^{\circ}\text{C}/\text{km}$  mentioned before to display a zonal character as well. It stretches from  $34^{\circ}\text{S}$   $22^{\circ}\text{W}$  to beyond the region of interest at the Greenwich meridian and  $39^{\circ}\text{S}$ . The region of homogenous water is again evident to the south-west of Gough Island centred at  $42^{\circ}\text{S}$  and  $13^{\circ}\text{W}$ . This was found to not be the only region exhibiting a near zero rate of change. It is situated even further southeast, centred at  $47^{\circ}\text{S}$  and  $16^{\circ}\text{W}$ . The most dominant feature once again is the region at  $42^{\circ}\text{S}$  to  $46^{\circ}\text{S}$ , associated with the SAF.

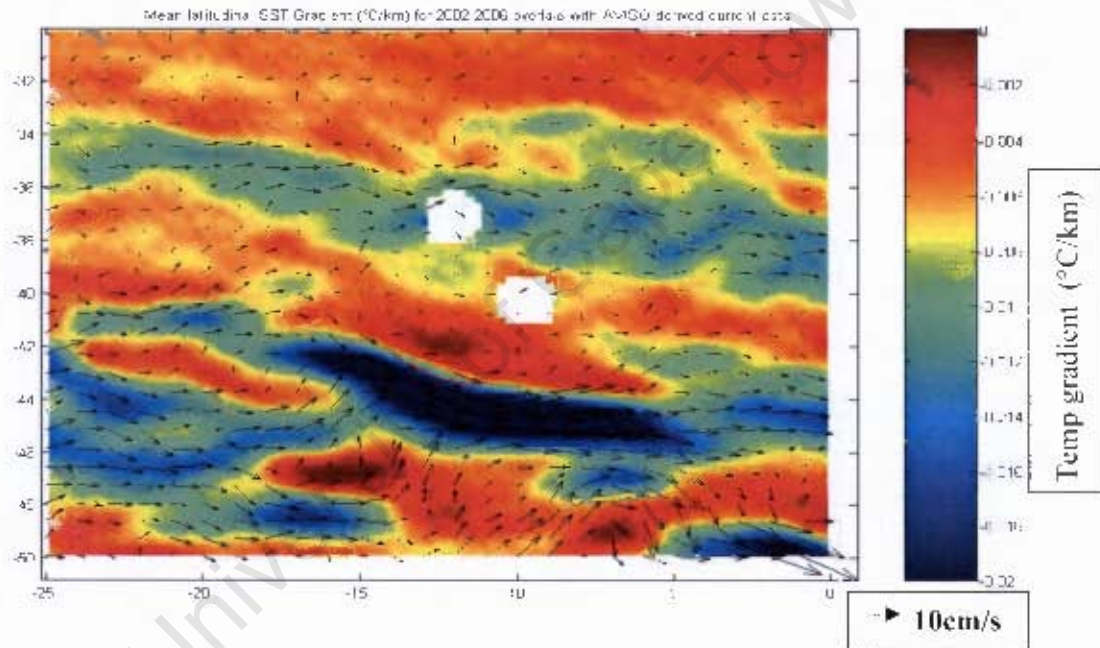


*Figure 16* Mean latitudinal AMSR SST gradient overlaid with AVISO derived current data

Burles and Reason (2006) found that regions with SST gradients greater than  $0.02^{\circ}\text{C}/\text{km}$  were associated with strong geostrophic flow. Mean altimetry derived geostrophic current data have been overlaid over the latitudinal temperature gradients in Figure 16. The region at  $42^{\circ}\text{S}$  to  $46^{\circ}\text{S}$  coincides with surface speeds of over  $25\text{cm}/\text{s}$ . The  $0.012^{\circ}\text{C}/\text{km}$  gradient was found to be consistent with speeds of between

15 and 20cm/s. The AVISO derived current is investigated in more detail in the following chapter.

### 3.3. Comparison of SODA current to AVISO data

Numerical models of ocean environment simulations are increasingly used to make up for the lack of in-situ data in certain areas.

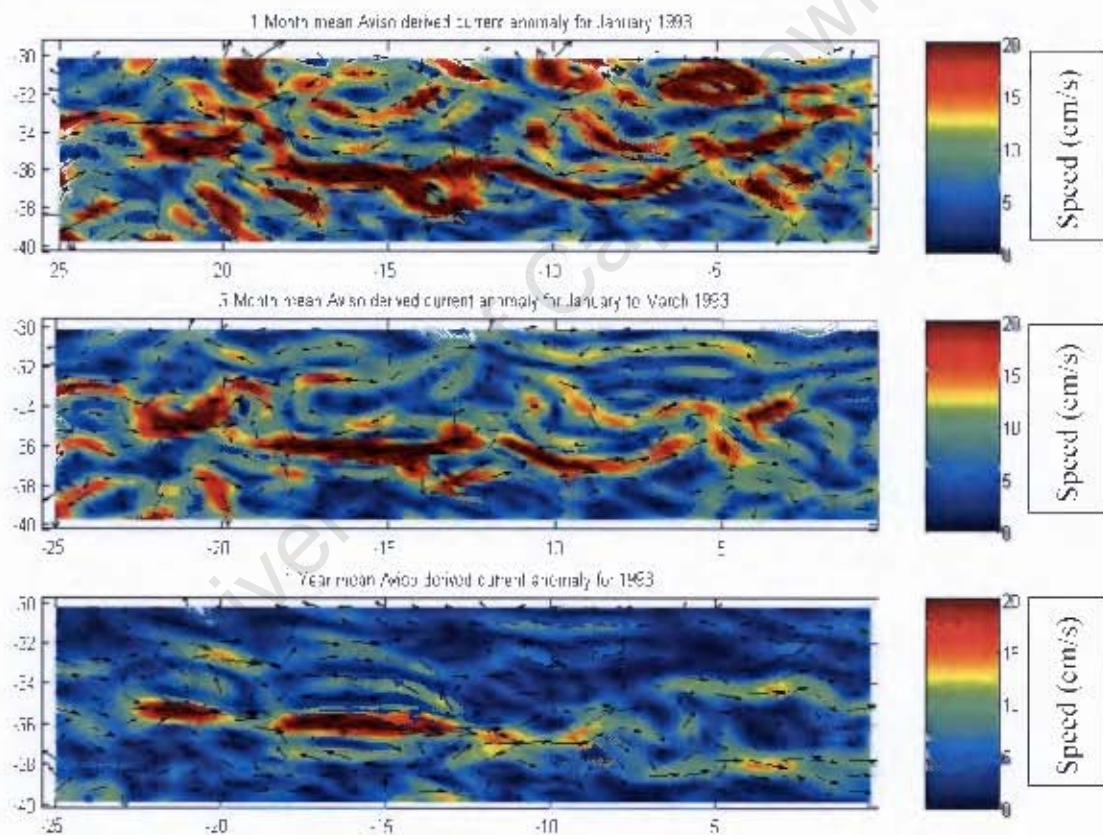


Figure 17 1 month (top); 3 month (middle); and 12month (bottom) mean AVISO derived geostrophic currents in cm/s for 1993

The AVISO derived geostrophic currents are used to describe the surface expression of the SAC. The SAC is identifiable, as is evident in Figure 17. A 1-month mean of

January 1993 (Figure 17 top) shows the strong westerly flow at 37°S. Just to the north a strong eddy field exists, which still greatly influences the 3-month mean taken from January to March 1993 (Figure 17 middle). The magnitude of speed of flow decreases as the means are taken over longer periods, for example, over 1 year (Figure 17 bottom). Here the general position is nearly as that depicted in the long term mean, shown in Figure 18.

To identify the validity of the SODA model in the region of interest, the model computed currents are compared to altimetry derived geostrophic current. A smaller region was chosen to better show smaller scale changes, possibly due to bathymetry.

The AVISO mean (Figure 18) shows a current flowing eastward at approximately 36°S. Immediately after Mid-Atlantic Ridge, the current shifts southward (right) as it flows over deeper regions to the east of the ridge. As it flows past Tristan da Cunha, it appears to have a slight change in direction northward (left) as it briefly crosses an area of decreased depth, and then corrects itself back slightly southeast-ward to regain its original flow from before it encountered the island. Another flow slightly further south, along approximately 40°S, exhibits similar properties except it undertakes a southward deflection.

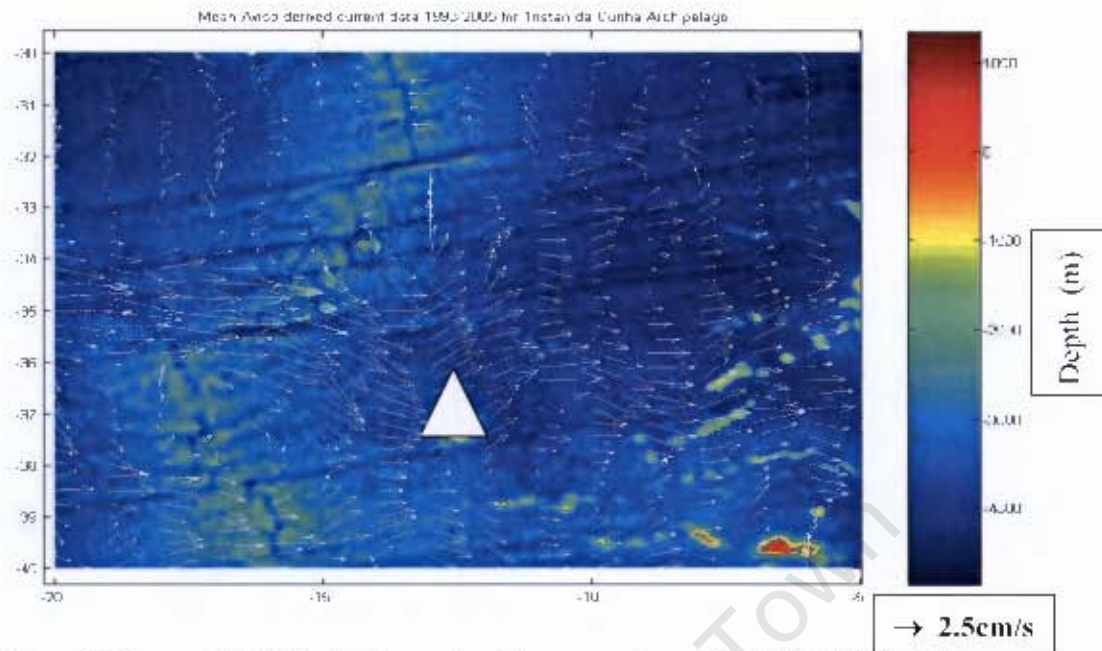


*Figure 18* Mean AVISO derived geostrophic current for period 1993-2005 at the Tristan da Cunha Archipelago with Etopo2v2 bathymetry as background. The light green area on the left side in the Figure represents the Mid-Atlantic Ridge, while the white triangle in the centre incorporates Tristan da Cunha, Nightingale and Inaccessible Islands. The dark orange regions on the right are shallow seamounts. On average, the depth in the region of interest is in excess of 3000m, depicted as dark blue here.

To compare the AVISO geostrophic current with the results from the SODA model output, the current layer at 96m was chosen (Figure 19) to decrease the effect of surface wind drift evident in shallower surface layers. Here, one cannot directly distinguish the dominant current at 36°S as one can in Figure 18, as the current is much weaker with values of 1cm/s. Although flowing much weaker, one can still recognise the slight change in direction of flow as it crosses areas both deeper (southward) and shallower (northward), as seen in the AVISO current in Figure 18.

There appears to be some form of current flowing eastward at 40°S. This does not match up with the results obtained by the altimetry-derived current.

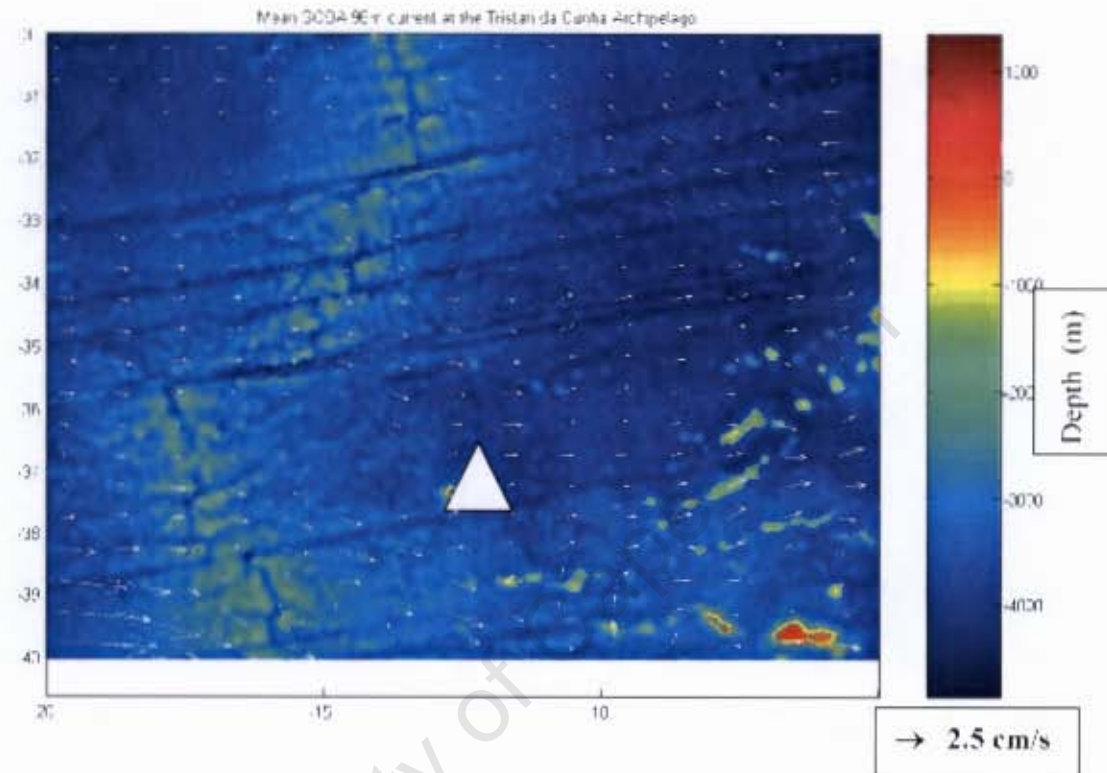


*Figure 19* Mean SODA current at 96m for period 1993-2005 at the Tristan da Cunha Archipelago with Etopo2 bathymetry as background, same as in Figure 18.

Probable causes are discussed in chapter 4



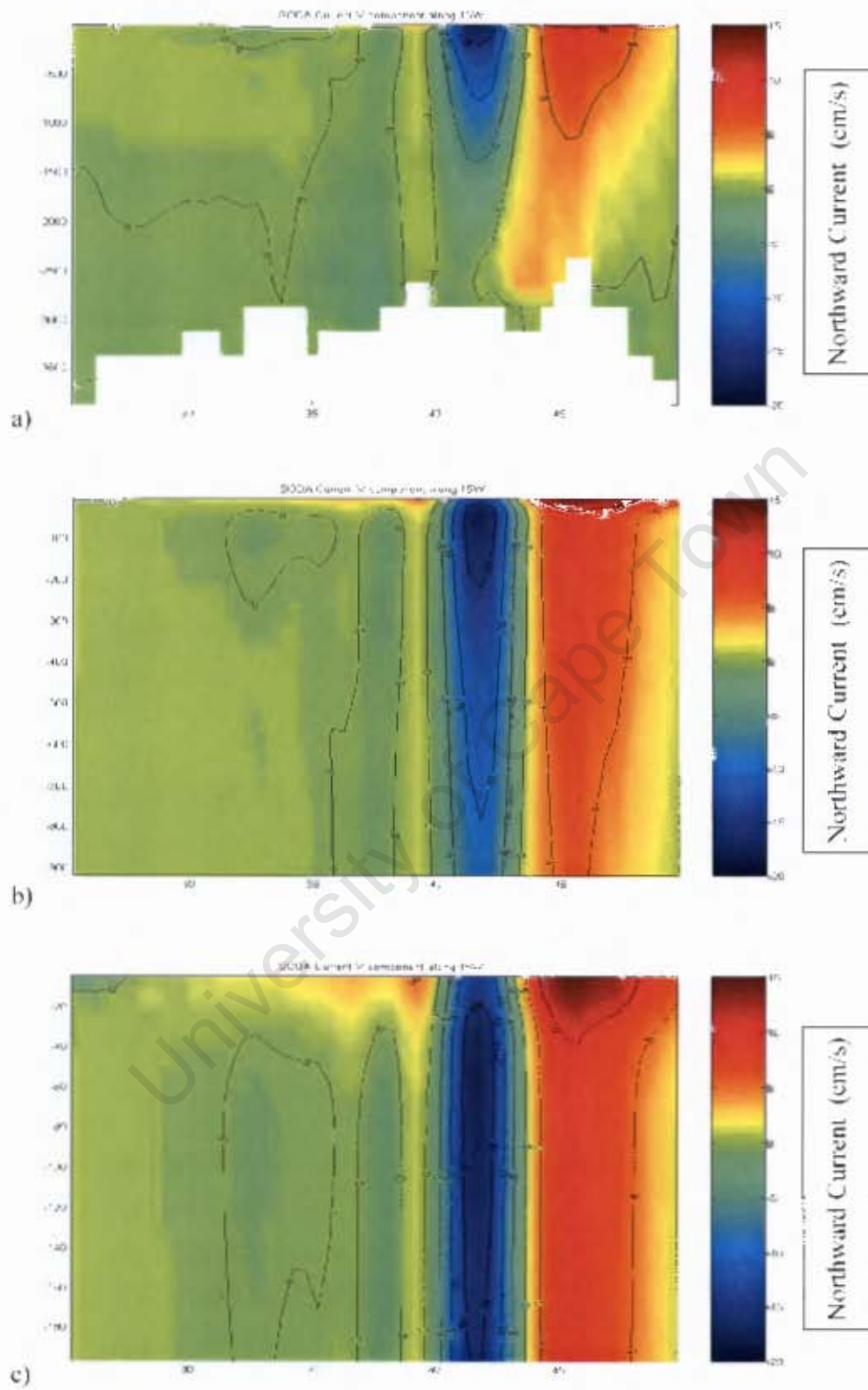


*Figure 20* Mean sub-surface SODA V-current component data in cm/s at 15°W for a) total water column, b) top 1000m and c) top 200m

To try understand the geostationary forcing of the Sub Antarctic Front (SAF) associated feature clearly evident in Figure 16 (Page 43) to the south of Gough, the south-north movement is investigated in Figure 20. A latitudinal section at 15°W was chosen, immediately downstream of the Mid-Atlantic Ridge. Using the V-component output of the SODA reanalysis model, a strong southward movement is evident at 42°S with values in excess of 15cm/s in an area of greater depth than over the ridge. Contrary, 3 Degrees south of this feature, centred at 45°S, a northward movement of over 10cm/s is present in an area shallower than that of the southward movement to the north. Both of these flows are found to extend all the way to the bottom (Figure 20a). In the region of 37°S there is minimal south-north movement, indicative of a near perfect zonally flowing SAC.

Comparing all surface layer data, namely temperature (Figure 8c, Page 33), salinity (Figure 9c, Page 35), U-current component (Figure 10c, Page 36) and V-current component (Figure 20c, Page 48), it becomes evident that all images display steep latitudinal gradients at 42°S.

### 3.4. Forcing of a cold event

The last question to be addressed in this study relates to anomalous events at the Tristan da Cunha Archipelago. Increased knowledge of unusual events in the central South Atlantic is not only important to the fragile fishing industry of Tristan da Cunha, but also further afield, to the weather patterns over Southern Africa (Tyson and Preston-Whyte, 2000). Notably local fishermen on Tristan da Cunha claim changes in catches are due to cold water intrusions. Unfortunately there are no scientific data available to further study these claims as there are no dates for these supposed events.

To identify an anomalous event, the normalised SST anomaly was calculated for Tristan da Cunha and Gough Island from OISST data. The criteria for an anomalous event were chosen to be an event that exceeded two standard deviations and lasted for longer than three months, to differentiate it from the short-term anomalous events caused by atmospheric variability. From the Gough Island in-situ SST dataset, six anomalous events were discovered. OISST data yielded four events for Gough Island and only one for Tristan da Cunha. No warm event that fulfilled the criteria was found at Tristan da Cunha. Of those found at both islands, only one was evident in all three extracted datasets. January to May of 1992 was of such a scale that it was experienced at both islands for duration of over three months.

<b>Warm events</b>			
<b>Location</b>	<b>Gough Island</b>	<b>Gough Island</b>	<b>Tristan da Cunha</b>
Data Source	In-situ data	OISST	OISST
	Jan 74 to Apr 74	Mar 82 to May 82	None longer than 3 months
	Dec 89 to May 90	Jan 00 to Mar 00	
	Mar 95 to Jul 95		
<b>Cold events</b>			
<b>Location</b>	<b>Gough Island</b>	<b>Gough Island</b>	<b>Tristan da Cunha</b>
Data Source	In-situ data	OISST	OISST
	May 64 to Jul 64	Jan 92 to June 92	Jan 92 to Apr 92
	Jan 67 to May 67	Mar 03 to May 03	
	Jan 92 to Apr 92		

*Table 3* Anomalous SST events at the Tristan da Cunha Archipelago

The cold event of 1992 was the strongest anomalous event from the OISST dataset (Box in Figure 21), being over 3 standard deviation out from the normalised mean, and covered an area in the South Atlantic extending from 30° to 50°S and 25°W to 5°E (Figure 22). The most pronounced anomaly region is situated just downstream of the Tristan da Cunha Archipelago showing over 1.5 standard deviation from the normalised mean.

The temperature experienced was not the coldest on record, 10.4°C during March 1992, as it occurred during late summer and early spring, and as such was just anomalous for that season and not the region as a whole, which was 9.9°C experienced during October 2001

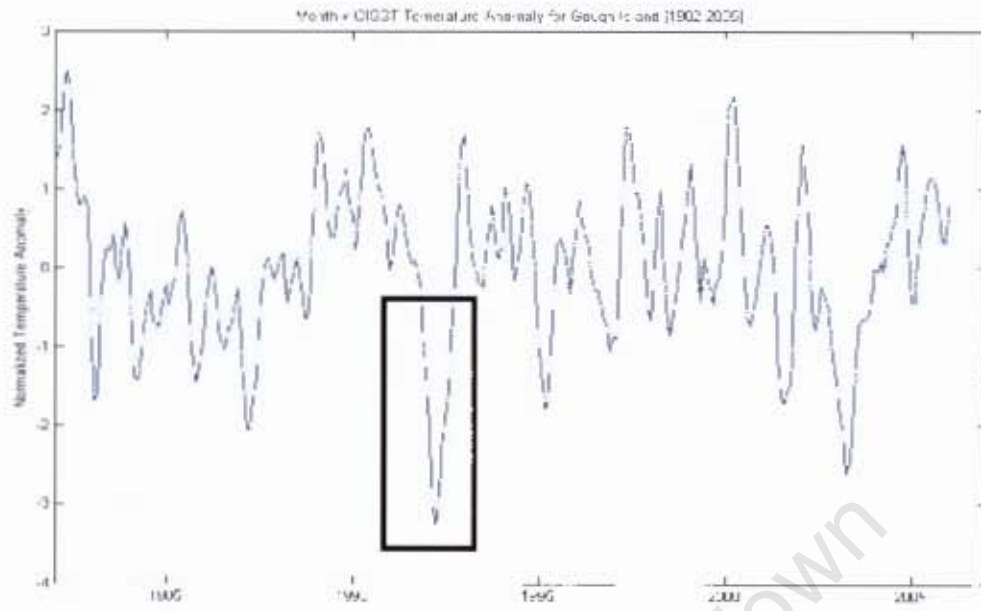


*Figure 21* Normalised OISST anomaly at Gough Island 1982-2005

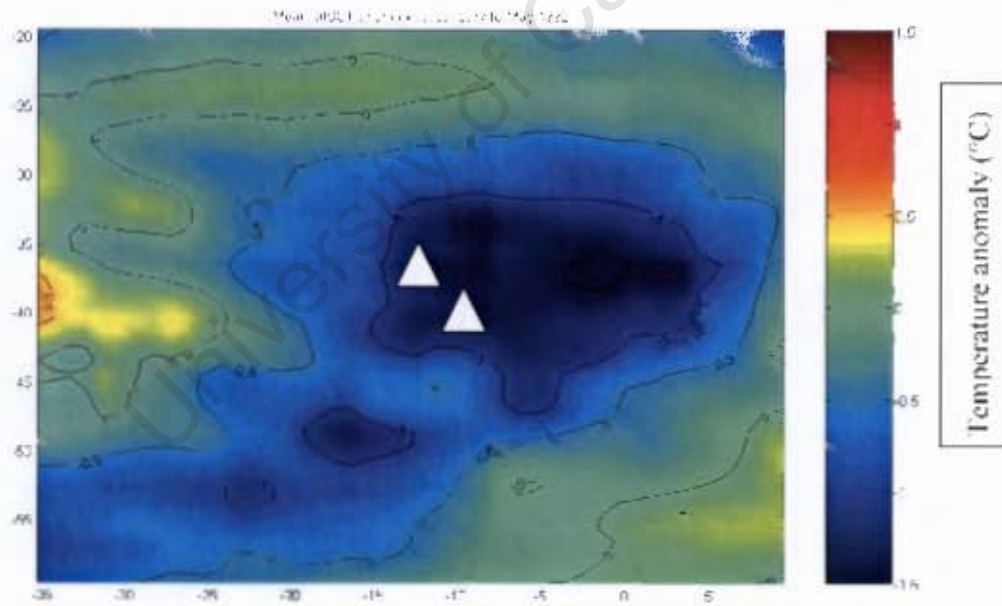


*Figure 22* Normalised OISST anomaly in °C at Tristan da Cunha Archipelago for January to May 1992

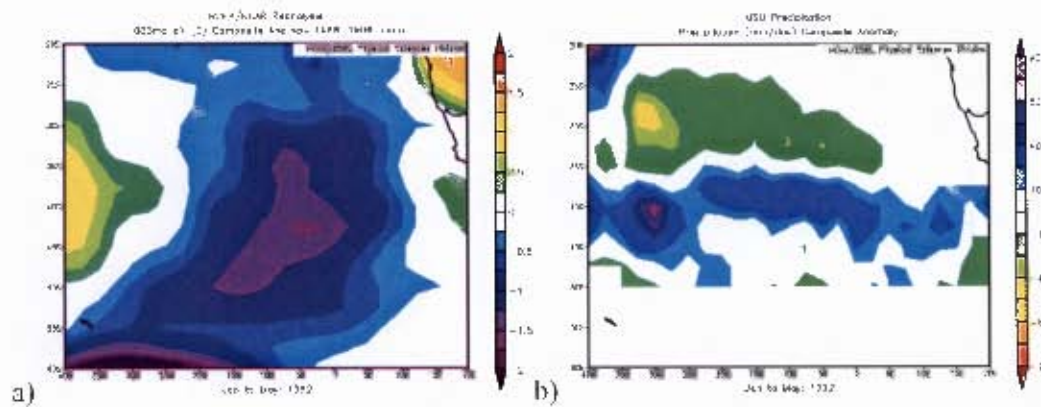
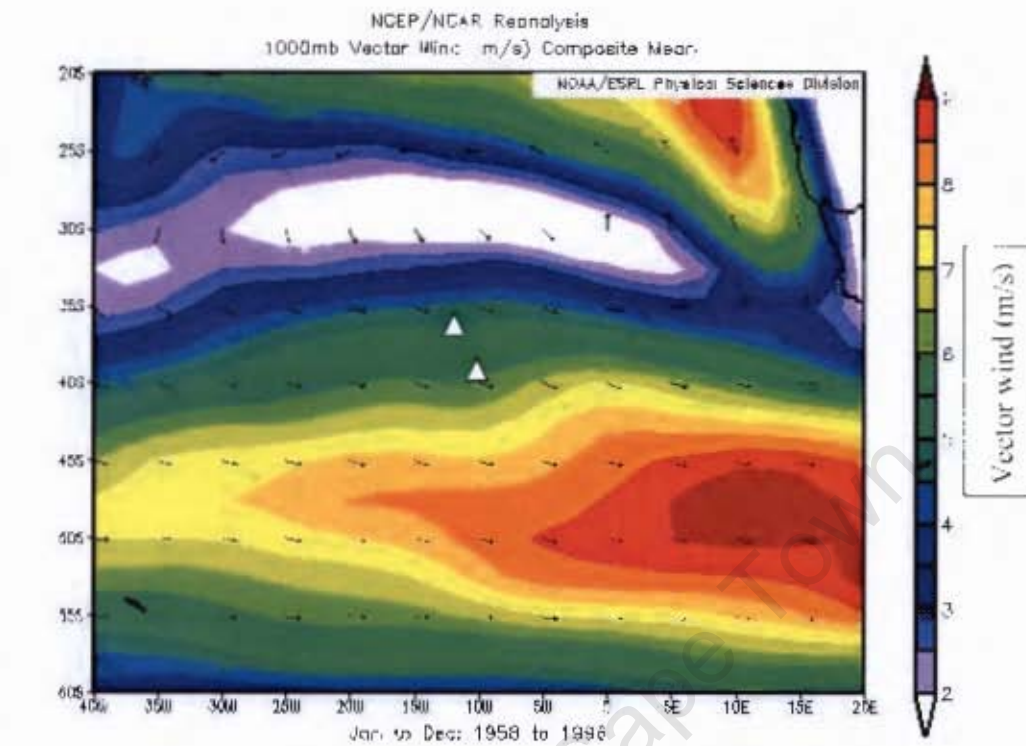


Figure 23 Air temperature (a) and precipitation (b) anomaly at Tristan da Cunha Archipelago for January to May 1992 obtained from the CDC website.

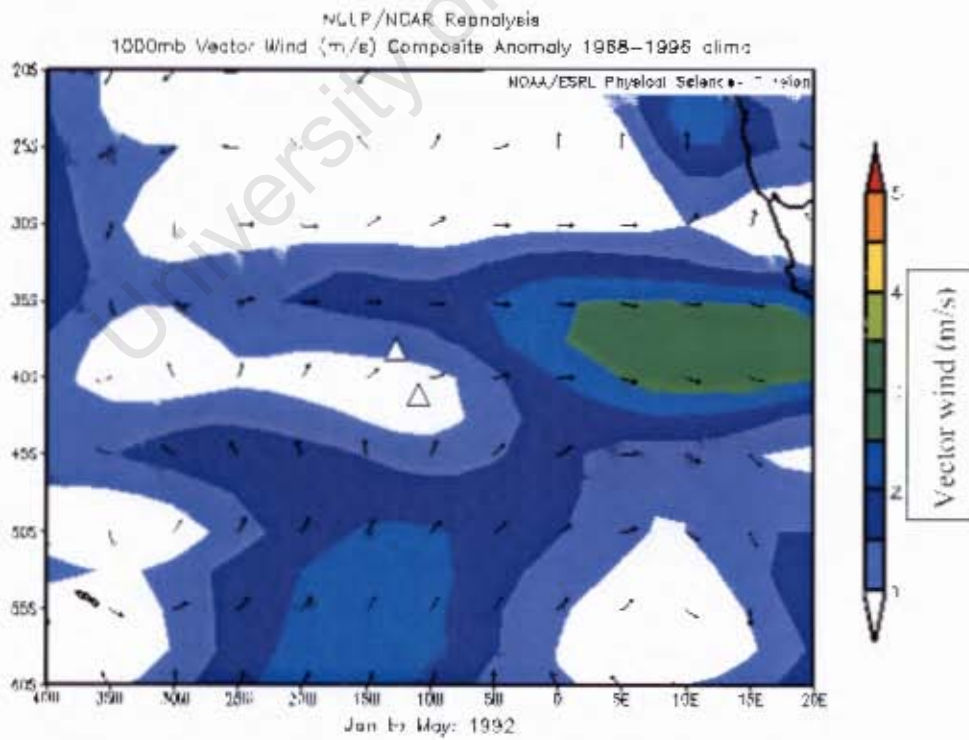
Also evident with the cold event was an air temperature anomaly of over 2°C colder for the region as well as a precipitation anomaly with more than 40mm of rain extra rain per day during that period (Figure 23 a and b) suggesting increased cloud coverage.

Figure 24 depicts a composite wind mean (Figure 24a). The mean depicts a westerly to northwesterly wind dominant for the region. More specifically in Figure 24b for the year 1992, the mean anomaly is southerly with approximately 2m/s associated anomalous wind speed.

Figure 25 shows the anomaly for all the El Niño years (obtained from the Climate Diagnostic Centre website ([www.cdc.noaa.gov](http://www.cdc.noaa.gov), August 2007) using years from the Niño 3.4 Index time series available on the site) for wind (Figure 25a) and precipitation rate (Figure 25b). In the region of interest around the Tristan da Cunha Archipelago, the wind anomaly shows a weak, but yet still evident, southerly anomalous wind up to 0.3m/s, whereas the precipitation rate is in excess of 0.1mm/day higher during El Niño years.



a)



b)

Figure 24 NCEP Mean wind (a) and anomaly for 1992 (b)

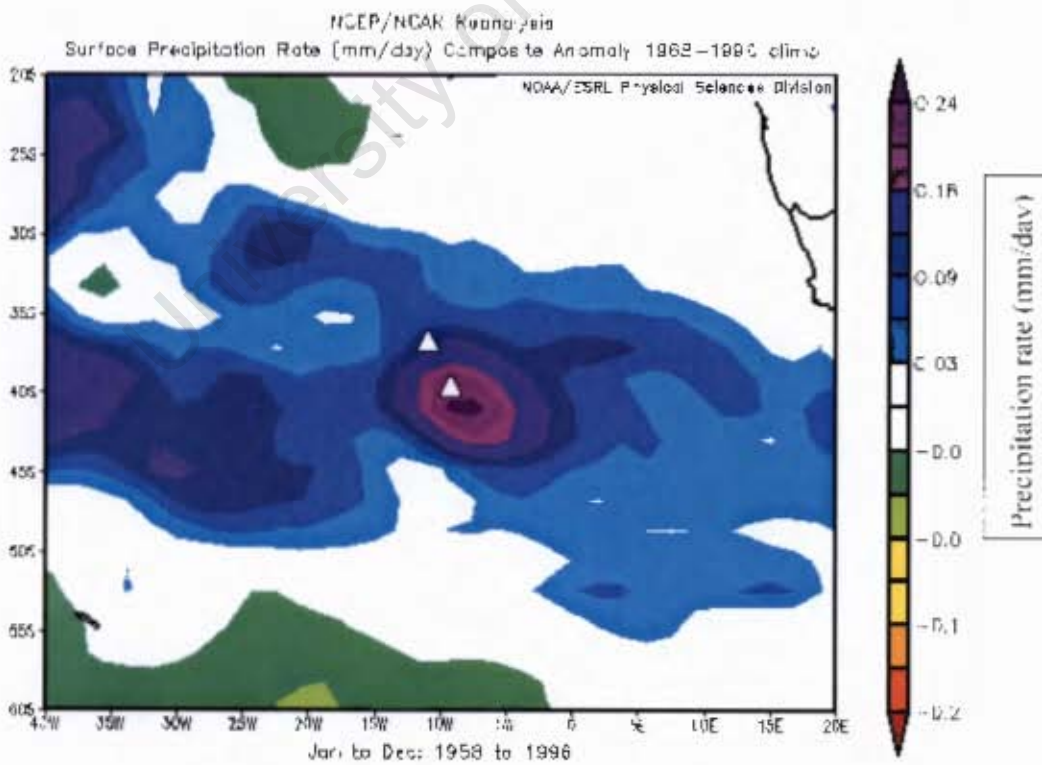
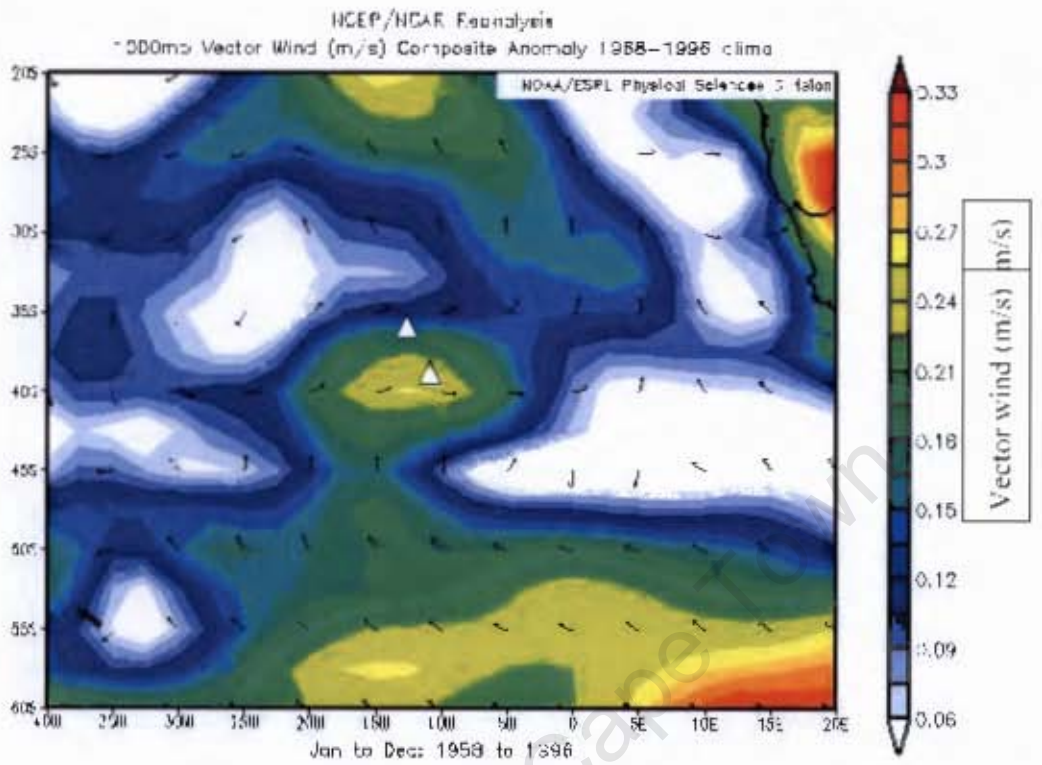


Figure 25 NCEP anomaly for all El Niño years for wind (a) and



## Precipitation rate (b)

### - Chapter 4 DISCUSSION and CONCLUSION

This study aimed to evaluate the seasonality of the STF, compare AVISO geostrophic currents with the SODA model and identify the probable cause of cold events in the central South Atlantic, with specific emphasis on the Tristan da Cunha Archipelago due to its importance to prevailing weather pattern over Southern Africa (Tyson and Preston-Whyte, 2000).

#### - 4.1.1. Seasonality of the STF

Comparing OISST with in-situ SST measurements yielded a  $0.28^{\circ}\text{C}$  mean difference. Rouault and Lutjeharms (2003) found a very similar result when comparing microwave Tropical Rainfall Measuring Mission (TRMM) data to OISST data over the Agulhas current. Although their global comparison only showed a  $0.18^{\circ}\text{C}$  difference, the Agulhas comparison yielded  $0.3^{\circ}\text{C}$ . Both of these observations fall in line with Rayner *et al.* (2002) who calculated that the OISST version 2 dataset was different by up to  $0.5^{\circ}\text{C}$  in the mid to high latitudes in the Southern Ocean.

Table 1 showed us that there is no set value for STF identification but rather a range of temperatures assigned to it during different times of the year. Smythe-Wright *et al.* (1998) argued that the use of a single isotherm could over-emphasise the zonal variability of the STF, as these could rather be due to insolation stratification, or mixing. The region exhibiting a temperature gradient of  $0.012^{\circ}\text{C}/\text{km}$  in Figure 14 (Page 41) most closely matches up with the previous literature written about the

location around the STF (Shannon *et al.*, 1989; Stramma and Peterson, 1990; Peterson and Stramma, 1991; Lutjeharms *et al.*, 1993; Smythe-Wright *et al.*, 1998; Mercier *et al.*, 2003). Other literature that used temperature gradients to identify the STF included Burls and Reason (2006) for the South Atlantic, Ullman *et al.*, (2007) for the North Atlantic and Kostianoy *et al.*, (2004) for the Indian Ocean.

The 6° latitudinal variation, as described by Deacon (1937), is only possible on an inter-annual timescale, as total seasonal latitudinal variation did not exceed 3° at 11°W. As was previously described by Stramma and Peterson (1990) the STF lay most commonly to the north of 40°S in the region between 25°W and Greenwich meridian.

Using the 0.012°C/km gradient as an indicator, the width of the STF band would be 333km on average. This is larger than the 120km width found during January 1984 (Whitworth and Nowlin, 1987) and the 220km width found to the south of South Africa (Lutjeharms and Valentine, 1987) and could be due to the rather coarse resolution of the OISST reanalysis as opposed to the higher resolution hydrographic data. The mean AMSR derived latitudinal temperature gradient at 11°W is slightly higher at 0.015°C/km, and would result in a width of 266km on average. The relatively narrow STF band to the south of Africa has been described as being one of the strongest latitudinal temperature gradients, and is most probably caused by the proximity of the continent (Lutjeharms and Valentine, 1987).

The strong current evident in a 13year mean just to the north of the Tristan da Cunha Archipelago can be associated with the South Atlantic Current (SAC). The SAC has

been described to be flowing between the NSTF and the SSTF (Smythe-Wright *et al.*, 1998). Speeds were found to be in the range of 15-20cm/s. Speeds of higher than 25cm/s were only found in the region exhibiting strong latitudinal temperature gradient at 42° to 46°S. Roden's (1986) estimate of 26cm/s for the SAC could have been mistaken for this region, which is more associated with the SAF (Burls and Reason, 2006). Studies of possible effects of the STF on the marine and bird life have been linked directly to the STF rather than the SAC (Andrew *et al.*, 1995; Barange *et al.*, 1998; Froneman *et al.*, 1997; Cuthbert *et al.*, 2005).

- 4.1.2. AVISO geostrophic currents in the South Atlantic and comparison to SODA

A comparison was attempted between SODA current data and AVISO altimetry derived currents. The AVISO showed strong currents at the surface with a high degree of spatial variability. At 96m the mean SODA current showed a degree of similarity with the mean AVISO current. Both show an extent of re-circulation northeast ward into Subtropical Gyre, starting at 10°W. Mercier *et al.* (2003) reported this re-circulation northwards to be of  $10 \pm 5$  Sv at 35°S.

No small-scale flow disturbance such as eddies due to bathymetry of the Tristan da Cunha Archipelago was directly evident from AVISO, unlike as was found in the vicinity of an isolated, deep ocean island off Australia's east coast where a surface-intensified cyclonic eddy in the wake intensified upwelling (Coutis and Middleton, 1999). An eddy would be clear in all the subsurface layers. This could be due to the relative sparse  $\frac{1}{2}^\circ$  resolution of the SODA model which would not represent smaller

scale changes. Also, averaging over a 13 year period could eliminate small-scale flow disturbances such as eddies.

Contrary however, on a larger scale, a flow disturbance possibly due to changes of bathymetry is evident just downstream of the Mid-Atlantic Ridge, as the current changes direction to the north (left) over shallower regions and south (right) over deeper regions.

In the vicinity of Tristan da Cunha, at 37°S 12°W, the flow downstream is disturbed and takes the appearance of a bifurcated current. This would prove Stramma and Peterson's (1990) theory of slowing down at the mid-ocean ridge for the year of 1993. Taking the mean over an extended number of years (Figure 18) does little to smooth out this occurrence, suggesting some form of bathymetric forcing.

The strong flow visible at 40°S in nearly all SODA depth layers (Figure 19) was found to coincide with the region of strong temperature gradient found at 42°S in AVISO, AMSR and OISST datasets. However there seems to be an overestimate of its northward extension in the SODA model reanalyses data.

Further westward at the Mid-Atlantic Ridge (Figure 20a) a south-north movement of water that extends all the way to the bottom is evident. A southward flow at 42°S and a northward flow at 45°S would cause a convergence of water masses, resulting in strong gradients, as is clearly visible in the temperature (Figure 8c) and salinity (Figure 9c) plots. This south-north movement seems to originate at approximately 15°W and is possibly brought about by topographical forcing.

- 4.1.3. Cold event of 1992

The NOAA run Climate Prediction Centre

([www.cpc.ncep.noaa.gov/products/analysis\\_monitoring/ensostuff/ensoyears.shtml](http://www.cpc.ncep.noaa.gov/products/analysis_monitoring/ensostuff/ensoyears.shtml),

January 2009) defines an El Niño event to be “a warm episode based on a threshold of +/- 0.5°C for the Oceanic Niño Index (ONI) [3 month running mean of ERSST.v3b SST anomalies in the Niño 3.4 region (5°N-5°S, 120°-170°W)], based on the 1971-2000 base period”. It is generally accepted that 1992 was an El Niño year as it fulfils the criteria from approximately mid 1991 to mid 1992.

Colberg *et al.* (2004) identified that some SST anomalies in the South Atlantic occur during El Niño and La Niña events, which could indicate a possible relationship through atmospheric forcing, rather than intrusion of cold waters. The cold event of 1992 coincided with anomalous southerly winds occurring during the early summer months as well as an increased precipitation rate over the south western part of the region of interest. The cold SST anomaly was not the coldest waters experienced in the region of interest, but rather became apparent due to the fact that it occurred in summer, a usually warm period. Colder surface waters from the south could have been blown northwards by the wind rather than the northward movement of the STF and intruded into the region of the Tristan da Cunha Archipelago. These anomalous winds appear to be linked to El Niño. From a mean of anomalous winds for the South Atlantic for all El Niño years (Figure 25a), one can deduce that these are the prevailing wind conditions during an El Niño event. These are again evident for a mean of January to May for 1992 from NNR winds (Figure 24b). Marshall (2003) reported that NNR winds were more accurate at 40°S, while ERA-40 winds better represented the region at 65°S. Increased precipitation rate during the El Niño years

(Figure 25b) over the region of interest centred on the Tristan da Cunha Archipelago would also have led to colder temperatures, suggesting increased cloud cover during the cold event observed during 1992. The precipitation anomaly is also found during the cold event year of 1992. The increase in precipitation might be linked to the southerly anomalous wind, which would bring colder air from the south into a region warmer air, resulting in frontal rain and cloud cover. No direct link was identified but rather potential causes that might have led to the cold event were highlighted.

#### 4.2. Conclusions

New data sets that reduce the need for in-situ hydrographic data are constantly being developed. Satellite data cover the ocean's entire surface, while numerical model simulations attempt to reconstruct the sub-surface environment. These models need to be scrutinised to confirm their validity. Anomalous events can have severe adverse affects on a wide variety of parameters and need to be properly understood to gain a better understanding of their forcing and effects. These were the main focus points of this study and were briefly investigated. More studies into these fields are still necessary to completely understand the complex environment that the oceans provide. The seasonality of the STF was investigated using primarily OISST and AMSR-E satellite data. The convention to assign a certain value to a particular front has again been brought into question in this research. With the recent introduction to study oceanfronts from satellite datasets over a longer period has resulted in adapting new methods to identify surface expressions. Definitions at the traditional 200m depth will remain, but the surface definitions will have to be refined. Using Deacon's (1937) assigned temperature change of 4°C in surface temperature, one can suggest an actual

value for the region over which the temperature changes. A gradient of  $0.012^{\circ}\text{C}/\text{km}$  was found to most closely represent the region associated with the STF.

Shortcomings in in-situ hydrographic data are increasingly covered by using numerical model simulations. These models however still need to be inspected to show that they represent the actual oceanographic environment. The SODA model was found to have an inaccuracy at the surface levels with regards to multiple satellite-derived surface products. The model was found to not be good for smaller scale studies, but very helpful to represent the bigger picture, such as bifurcation of the current. The region at  $42^{\circ}\text{S}$  exhibited strong current flow and intense latitudinal temperature and salinity gradient and might be the result of flow disturbance due to the Mid-Atlantic Ridge. This region was not the focal point of this research, and has as yet still needed to be firmly identified in all oceanographic aspects. The SAC was also found to not be a definite current but rather a short-lived one which is mostly only clearly visible in mean composites spanning several months.

The far-reaching effect of El Niño is still unknown in open ocean regions, specifically over the South Atlantic. With regards to SST anomalies and a possible link to ENSO, one such event was found. The evidence of a cold water intrusion found could rather be due to atmospheric forcing than due to the movement of the STF. The possible forcing included changes in wind-driven surface water as well as increased precipitation rate along with related cloud cover reducing solar radiation to the region. The increased rainfall might be due to the anomalous southerly wind advecting colder air from the south into a region of warmer air creating frontal rainfall and cloud cover. ENSO induced SST anomalies were not evident during every event and so a direct link cannot be assumed between South Atlantic SST. A study by Colberg *et al.* (2004) estimated at least a one-year lag.

South Atlantic variability is still only weakly understood and a lot of research still needs to be undertaken to better understand the variability on interannual and multidecadal timescales (Colberg *et al.*, 2004). To overcome the sparseness of data Campos *et al.* (1999) have asked for a reoccupation of the WOCE lines in the South Atlantic.

University of Cape Town



## REFERENCES

- Andrew, T.G., Hecht, T., Heemstra, P.C. and Lutjeharms, J.R.E., 1995, Fishes of the Tristan da Cunha Group and the Gough Island, South Atlantic Ocean, *Ichthyological Bulletin of the J.L.B Smith Institute of Ichthyology*, 63, 41 pages
- Barange, M., Pakhomov, E. A., Perissinotto, R., Froneman, P. W., Verheye, H. M., Taunton-Clark, J., Lucas, M., 1998, Pelagic community structure of the Subtropical convergence region south of Africa and in the mid-Atlantic Ocean, *Deep Sea Research Part I*, 45, 1663-1687
- Belkin, I.M. and Gordon, A.L., 1996, Southern Ocean fronts from the Greenwich meridian to Tasmania *Journal of Geophysical Research*, 101, 3675-3696
- “5” Berger, W., Wefer, G., 1996, Central themes of the South Atlantic circulation, in: Berger, W., Wefer, G., Siedler, G., Webb, D., (Eds), *The South Atlantic: Present and Past Circulation*, Springer Verlag, Berlin, 1996, pp.1-11.
- “1” Burling, R.W., 1961, Hydrology of circumpolar waters south of New Zealand, *N.Z. DSIR Bull.*, 143, 66pp
- Burls N.J., Reason C.J.C., 2006, Sea surface temperature fronts in the mid latitude South Atlantic revealed by using microwave satellite data, *Journal of Geophysical Research*, Vol. 111, C08001, doi:10.1029/2005JC003133

Campos, E.J.D., Busalacchi, A., Garzoli, S., Lutjeharms, J., Matano, R., Nobre, P., Olson, D., Piola, A., Tanajura, C., and Wainer, I., 1999,: The South Atlantic and the Climate. *Invited paper to the OCEANOBS99, St. Raphael, France, Oct. 1999.*  
[http://www.labmon.io.usp.br.iaii\\_papers/oceanobs99/](http://www.labmon.io.usp.br.iaii_papers/oceanobs99/)

Carton, J.A., Chepurin, G., Cao, X.H., Giese, B., 2000a, A Simple Ocean Data Assimilation analysis of the global upper ocean 1950-95. Part 1: Methodology, *Journal of Physical Oceanography, Vol. 30, 2, 294-309*

Carton, J.A., Chepurin, G., and Cao, X. 2000b: A Simple Ocean Data Assimilation analysis of the global upper ocean 1950-1995 Part 2: results, *J. Phys. Oceanogr.*, **30**, 311-326.

“I” Clifford, M.A., 1983, A descriptive study of the of the zonation of the Antarctic Circumpolar Current and its relation to wind stress and ice cover, M.S.thesis, 93pp., Texas A&M Univ., College Station

Colberg, F., Reason, C.J.C., Rogers, K., 2004, South Atlantic response to El Niño-Southern Oscillation induced climate variability in an ocean general circulation model, *Journal of Geophysical Research, Vol. 109, C12015*,  
doi:10.1029/2004JC002301

Coutis, P.F., Middleton, J.H., 1999, Flow-topography interaction in the vicinity of an isolated, deep ocean island, *Deep Sea Research I, Vol. 46, 1633-1652*

Cuthbert, R., Hilton, G., Ryan, P., Tuck, G., 2005, At-sea distribution of breeding Tristan albatrosses *Diomedea dabbenena* and potential interactions with pelagic longline fishing in the South Atlantic Ocean, *Biological Conservation*, Vol.121, 345-355

“1” Deacon, G.E.R., 1933: A general account of the hydrology of the South Atlantic Ocean, *Discovery Reports*, 7: 171-238

Deacon, G.E.R., 1937: The hydrology of the southern ocean, *Discovery Reports*, 15: 3-122

Deacon, G.E.R., 1982, , Physical and biological zonation of the Southern Ocean, *Deep Sea Research*, 29 (1A), 1-15

Emery, W.J., Brandt, P., Funk, A., Böning, C., 2006, A comparison of sea surface temperatures from microwave remote sensing of the Labrador Sea with in situ measurements and model simulations, *Journal of Geophysical Research*, Vol.111, C12013, doi:10.1029/2006JC003578

Froneman, P.W., Perissinotto, R., Pakhomov, E.V., 1997, Biogeographical structure of the microphytoplankton assemblages in the region of the Subtropical Convergence and across a warm-core eddy during austral winter, *Journal of Plankton Research*, Vol. 19, 519-531

Fyfe, J.C., 2006, Southern Ocean warming due to human influence, *Geophysical Research Letters*, Vol.33, L19701, doi:10.1029/2006GL027247

Garzoli, S.L., Richardson, P.L., Duncombe Rae, M., Fratantoni, D.M., Goñi, G.J., Roubicek, A.J., 1999, Three Agulhas rings observed during the Benguela Current Experiment, *Journal of Geophysical Research*, Vol.104, No.C9, 20971-20985

“6” Gordon, A.L., Weiss, R.F., Smethie, W.M. and Warner, M.J. (1992). Thermocline and intermediate water communication between the South Atlantic and Indian Oceans, *Journal of Geophysical Research*, Vol.97, 7223-7240

Hofmann, D.I., Fabian, K., Schmieder, F., Donner, B., Bleil, U., 2005, A stratigraphic network across the Subtropical Front in the central South Atlantic: Multi Parameter correlation of magnetic susceptibility, density, X-ray fluorescence and  $\delta^{18}\text{O}$  records, *Earth and Planetary Science Letters*, 240, 694-709

Isern-Fontanet, J., Chapron, B., Lapeyre, G., Klein P., 2006, Potential use of microwave sea surface temperatures for the estimation of ocean currents, *Geophysical Research Letters*, 33, L24608, doi:10.1029/2006GL027801

“3” Knox, G.A., 1960, Littoral ecology and biology of the Southern Ocean, *Proc. Roy. Soc. Lond(Ser.B)*. 152:577-624

“2” Krummel, O., 1882: Bemerkungen über die Meeresströmungen und Temperaturen in der Falklandsee, *Aus dem Archiv der deutschen Seewerte*, V(2), 25 pp.

Kostianoy, A.G., Ginzburg, A.I., Frankignoulle, M., Delille, B., 2004, Fronts in the South Indian Ocean as inferred from satellite sea surface temperature data, *Journal of Marine Systems*, 45, 55-73

Llido, J., Garçon, V., Lutjeharms, J.R.E., Sudre, J., 2005, Event-scale blooms drive enhanced primary productivity at the Subtropical Convergence, *Geophysical Research Letters*, Vol.32, L15611, doi:10.1029/2005GL022880

Lutjeharms, J.R.E., Valentine, H.R., 1987, Eddies at the Subtropical Convergence South of Africa, *Journal of Physical Oceanography*, Vol. 18, 761-774

Lutjeharms, J.R.E., Valentine, H.R., and van Ballegooyen, R.C., 1993, On the Subtropical Convergence in the South Atlantic Ocean, *South African Journal of Science*, 89, 552-559

"1" Lutjeharms, J.R.E., and Valentine, H.R., 1984, Southern Ocean thermal fronts south of Africa, *Deep-Sea Research I* Vol.31, 1461-1475

Marshall, G.J., 2003, Trends in the Southern Annular Mode from Observations and Reanalyses, *Journal of Climate*, Vol. 16, 4134-4143

Matano, R., Strub, T., James, C., 2003, The low-frequency variability of the South Atlantic circulation, *Geophysical Research Abstracts*, Vol.5, 03297

Melice, J-L., Lutjeharms, J.R.E., Rouault, M. and Ansorge, I., 2003, Sea-surface temperatures at the sub-Antarctic islands Marion and Gough during the past 50 years *South African Journal of Science*, 99, 363-366

Mercier, H., Arhan, M., Lutjeharms, J.R.E., 2003, Upper-layer circulation in the eastern Equatorial and South Atlantic Ocean in January-March 1995, *Deep-Sea Research I Vol.50*, 863-887

Miller, D.G.M., Tromp, B.B.S., 1982, The hydrology of waters close to Gough Island, *South African Journal of Antarctic Research, Vol. 12*, 23-33

“1” Nagata, Y., Michida, Y., and Umimura, Y., 1988, Variation of positions and structures of the oceanic fronts in the Indian Ocean sector of the Southern Ocean in the period from 1965 to 1987, *Antarctic Ocean and Resource Variability*, edited by D. Sahrhage, pp.92-98, Springer-Verlag, New York

“1” Orsi, A.H, Nowlin, W.D., Whitworth, T., 1993, On the circulation and stratification of the Weddell Gyre, *Deep Sea Res.*, 40, 169-203

“1” Orsi, A.H, Nowlin, W.D., Whitworth, T., 1995, On the meridional extent and fronts of the Antarctic Circumpolar Current, *Deep Sea Res.*, 42, 641-673

“1” Park, Y.H, Gambéroni, L., Charriaud, E., Frontal structure, water masses and circulation in the Crozet Basin, *Journal of Geophysical Research*, 98, 12,361-12,385

Peterson, R.G. and Stramma, L., 1991, Upper-level circulation in the South Atlantic Ocean, *Progress in Oceanography*, 26, 1-73

Peterson, R.G. and Stramma, L., Kortoum, G., 1996, Early concepts and charts of ocean circulation, *Progress in Oceanography*, 37, 1-115

Reason, C.J.C., Mysak, L.A., Cummins, P.F., 1987, Generation of Annual-Period Rossby Waves in the South Atlantic Ocean by the Wind Stress Curl, *Journal of Physical Oceanography*, Vol.17, 2030-2042

“4” Rennel, J., 1832 An investigation of the currents of the Atlantic Ocean, and of those which prevail between the Indian Ocean and the Atlantic. *J.G.&F. Rivington*, London, 359 pp., 2 plates.

Reynolds, R.W., 1988, A Real-Time Global Sea Surface Temperature analysis, *Journal of Climate*, Vol.1, 75-86

Reynolds, R.W., Rayner, N.A., Smith, T.M., Stokes, D.C., Wang, W., 2002, An improved in situ and satellite SST analysis for climate, *Journal of Climate*, Vol.15, 1609-1625

Roden, G.I., 1986, Thermohaline fronts and baroclinic flow in the Argentine Basin during the austral spring of 1984, *Journal of Geophysical Research*, 91, 5075-5093

Rouault, M., Lutjeharms, J.R.E., 2003, Estimation of sea-surface temperature around southern Africa from satellite-derived microwave observations, *South African Journal of Science*, Vol.99, 489-494

Rouault, M., Melice, J-L., Reason, C.J.C, and Lutjeharms, J.R.E, (2005) Climate variability at Marion Island, Southern Ocean, since 1960, *Journal of Geophysical Research*, 110

Shannon, L.V., Pollock, D.E., Chapman, P., Robertson, A.A., 1989, South-east Atlantic Expedition of R.S *Africana*, April 1989: some preliminary results, *S. Afr.J.Sci.* 85, 665-669

Smythe-Wright, D., Chapman, P., Duncombe Rae, C., Shannon, L.V. and Boswell, S.M., 1998, Characteristics of the South Atlantic subtropical frontal zone between 15°W and 5°E *Deep-Sea Research 1*, 45, 167-192

Sokolov, S., Rintoul, S., 2002, Structure of Southern Ocean Fronts at 140°E, *Journal of Marine Systems* 37, 151-184

Sterl, A., Hazeleger, W., 2003, Coupled variability and air-sea interaction in the South Atlantic Ocean, *Climate Dynamics*, 1-19

Stramma, L. and Peterson, R.G., 1990, The South Atlantic Current, *Journal of Physical Oceanography*, 20, 846-859



“1” Stramma, L. 1992, The South Indian Ocean Current, *Journal of Physical Oceanography*, 22, 421-430

Stramma, L. and England, M., 1999, On the water masses and the mean circulation of the South Atlantic Ocean, *Journal of Geophysical Research*, 104 (C9), 20,863-20,883

Sverdrup, H.U., Johnson, M.W., Flemming, R.H., 1942, The Oceans Their Physics, Chemistry, and General Biology, *Prentice-Hall, Engelwood Cliffs, New Jersey*

Tyson, P.D. and Preston-Whyte, R.A. (2000) The Weather and Climate of Southern Africa, *Oxford University Press Southern Africa*

Ullman, D.S., Cornillon, P.C., Shan, Z., 2007, On the characteristics of the subtropical fronts in the North Atlantic, *Journal of Geophysical Research*, Vol. 112, C01010, doi:10.1029/2006JC003601

Weeks, S.J., Shillington, F.A., 1996, Phytoplankton pigment distribution and frontal structure in the subtropical convergence region south of Africa, *Deep Sea Research, Part 1, Vol.43*, 739-768

Whitworth III, T., Nowlin, W.D., 1987, Water Masses and Currents of the Southern Ocean at the Greenwich Meridian, *Journal of Geophysical Research*, Vol. 92, No.C6, 6462-6476

Please Note:

References marked with a "1" where taken from the review article Belkin and Gordon (1996)

Reference marked with a "2" where taken from the review article Peterson *et al.* (1996)

Reference marked with a "3" where taken from the review article Andrew *et al.* (1995)

Reference marked with a "4" where taken from the review article Stramma and Peterson. (1990)

Reference marked with a "5" where taken from the review article Hofmann *et al.*. (2005)

Reference marked with a "6" where taken from the review article Lutjeharms *et al.*, (1993)

University of Cape Town